

INVESTIGATION OF THE EFFECT OF SODIUM BUTYRATE ON THE
REGULATION OF CYCLOOXYGENASE-2 IN COLON CANCER CELL
LINES CACO-2 AND HT-29

A THESIS SUBMITTED TO
THE GRADUATE SCHOOL OF NATURAL AND APPLIED SCIENCES
OF
MIDDLE EAST TECHNICAL UNIVERSITY

BY

DOĞUKAN HAZAR ÜLGEN

IN PARTIAL FULFILLMENT OF THE REQUIREMENTS
FOR
THE DEGREE OF MASTER OF SCIENCE
IN
BIOLOGY

FEBRUARY 2015

Approval of the thesis:

**INVESTIGATION OF THE EFFECT OF SODIUM BUTYRATE ON
THE REGULATION OF CYCLOOXYGENASE-2 IN COLON
CANCER CELL LINES CACO-2 AND HT-29**

submitted by **DOĞUKAN HAZAR ÜLGEN** in partial fulfillment of the requirements for the degree of **Master of Science in Biology Department, Middle East Technical University** by,

Prof. Dr. Gülbin Dural Ünver
Dean, Graduate School of **Natural and Applied Sciences** _____

Prof. Dr. Orhan ADALI
Head of Department, **Biology** _____

Assoc. Prof. Dr. Sreeparna Banerjee
Supervisor, **Biology Dept., METU** _____

Examining Committee Members:

Assoc Prof. Dr. Mesut Muyan
Biology Dept., METU _____

Assoc Prof. Dr. Sreeparna Banerjee
Biology Dept., METU _____

Assoc Prof. Dr. Can Özen
Biotechnology Dept., METU _____

Assoc. Prof. Dr. Mayda Gürsel
Biology Dept., METU _____

Assist. Prof. Dr. Ebru Erbay
Molecular Biology and Genetics Dept., Bilkent University _____

Date: 03/02/15

I hereby declare that all information in this document has been obtained and presented in accordance with academic rules and ethical conduct. I also declare that, as required by these rules and conduct, I have fully cited and referenced all material and results that are not original to this work.

Name, Last name: Dođukan Hazar Ülgen

Signature :

ABSTRACT

INVESTIGATION OF THE EFFECT OF SODIUM BUTYRATE ON THE REGULATION OF CYCLOOXYGENASE-2 IN COLON CANCER CELL LINES CACO-2 AND HT-29

Ülgen, Doğukan Hazar

M.S., Department of Biology

Supervisor: Assoc. Prof. Dr. Sreeparna Banerjee

February 2015, 103 pages

Sodium butyrate (NaBt) is a four-carbon short-chain fatty acid histone deacetylase inhibitor (HDACi) that is available in the colon through the commensal microbiota-mediated fermentation of dietary fibers. It is the main source of energy for colonocytes, and is regarded to have tumor suppressive effects, most prominently in colorectal cancer (CRC). Cyclooxygenase-2 (COX-2) is a gene important in the inflammatory response due to its ability to convert arachidonic acid to prostaglandins. Overexpression and overactivity of COX-2 were observed in chronic inflammatory diseases and CRC. To understand whether the expression of COX-2 was regulated through NaBt in CRC, we treated Caco-2 and HT-29 cells with 3mM NaBt. We observed that Caco-2 cells treated with 3 mM NaBt showed increased mRNA and protein expression of COX-2 while a decrease in the same was observed in HT-29 cells. To understand the mechanism behind this dual regulation, we analyzed the transcriptional regulation of COX-2 through NF- κ B. Contrary to our

expectations, we found that even though the nuclear localization of p65 subunit of NF- κ B showed an increase in Caco-2 cells and not in HT-29 cells, the recruitment of NF- κ B to the COX-2 promoter region decreased in Caco-2 cells, and increased in HT-29 cells. We therefore hypothesized that COX-2 was regulated post-transcriptionally. We observed that mitogen-activated protein kinase (MAPK) p38, a pathway that activates a number of proteins involved in mRNA stabilization, was activated only in Caco-2 cells and not HT-29 cells. We investigated the downstream signaling and discovered that the use of distal polyadenylation signal, and the stability of COX-2 were increased in NaBt-treated Caco-2 cells and decreased in HT-29 cells. We then showed that the said stability was lost when the p38 activity was inhibited in Caco-2 cells. The stabilizing AU-rich element binding protein (AREBPs) HuR was found to decline in the two cell lines, whereas destabilizing AREBP TTP exhibited a decrease only in Caco-2 cells. Collectively, this study indicates that NaBt can modify the transcriptome not only through its HDACi ability but also via the activation of p38-dependent post-transcriptional regulation networks.

Keywords: Sodium butyrate, cyclooxygenase-2, colorectal cancer, Caco-2, HT-29, inflammation, NF- κ B, post-transcriptional regulation, p38, HuR, TTP.

ÖZ

CACO-2 VE HT-29 KOLON KANSERİ HÜCRE HATLARINDA SODYUM BÜTİRAT MUAMELESİNİN SİKLOOKSİJENAZ-2 REGÜLASYONU ÜZERİNE ETKİSİNİN ARAŞTIRILMASI

Ülgen, Dođukan Hazar

Yüksek Lisans, Biyoloji Bölümü

Tez Yöneticisi: Doç. Dr. Sreeparna Banerjee

Şubat 2015, 103 sayfa

Sodyum bütirat (NaBt), kommensal mikrobiyotanın diyet liflerini fermentasyonu yoluyla kolonda ortaya çıkan, dört karbonlu bir kısa zincir yağ asidi olup aynı zamanda bir histon deasetilaz inhibitörüdür (HDACi). Kolonositlerin birincil enerji kaynağı olmasının yanısıra, özellikle kolorektal kanser üzerinde önemli tümör-baskılayıcı etkileri olduğu bilinmektedir. Siklooksijenaz-2 (COX-2), araşidonik asitten prostaglandin sentezini yönetmesinden dolayı, enflamatuvar tepkide önemli bir gendir, ve kronik enflamatuvar hastalıklar ve kolorektal kanserde overekspresyon ve overaktivitesi görülmektedir. İki farklı kolon kanseri hücre hattı olan Caco-2 ve HT-29'da, 3 mM NaBt muamelesinin, COX-2 mRNA ve protein seviyelerini farklı şekilde etkilediği bulgusunu elde ettikten sonra, bu regülasyonun ardında yatan mekanizmayı bulmak için çabaladık. NF-κB'nin p65 altbiriminin nükleer lokalizasyonunun Caco-2'de artmasına ve HT-29'da değişmemesine rağmen NF-κB'nin COX-2 promotoruna çağırılmasının Caco-

2'de azaldığı, HT-29'da ise arttığı sonucuna vardık. p38 proteininin, NaBt muamelesi sonucunda sadece Caco-2'de aktive edildiğini gördükten sonra, takip eden sinyal yollarını inceledik ve Caco-2 hücrelerinde, COX-2 mRNA'sının distal poliadenilasyon sinyali kullanımında ve stabilitesinde bir artış gözlemledik. Yine Caco-2 hücrelerinde, işbu stabilitenin, p38 aktivitesi inhibe edildiğinde yok olduğunu gösterdik. Stabilize edici AU-bölge bağlayıcı protein (AREBP) HuR'un seviyelerinin iki hücrede NaBt muamelesiyle azaldığı, ancak destabilize edici AREBP TTP seviyesinin sadece Caco-2 hücrelerinde azaldığını gözlemledik. Sonuç itibarıyla bu çalışma, NaBt'nin hücre transkriptomunu bilinen HDACi özelliğinin yanısıra, p38 aktivasyonu yoluyla beliren post-transkripsiyonel regülasyonlar aracılığıyla da etkilediğini göstermektedir.

Anahtar kelimeler: sodyum bütirat, siklooksijenaz-2, kolorektal kanser, Caco-2, HT-29, enflamasyon, NF- κ B, post-transkripsiyonel regülasyon, HuR, TTP.

To my family

ACKNOWLEDGEMENTS

I am deeply grateful to my supervisor Assoc. Prof. Dr. Sreeparna Banerjee for the guidance, comments and encouragement throughout this study. Without her belief and the support, I would never be able to pursue the scientific questions in my mind. I would also like to thank her for never getting bored (or at least never admitting to do so) of listening to my hypotheses over and over again.

I would like to thank Assoc. Prof. Dr. Ayşe Elif Erson Bensen for her guidance to the RNA biology and Assoc. Prof. Dr. Mesut Muyan for the brainstormings and the support in ChIP experiments.

I would like to express my gratitude to all of my dear current and ex-lab mates, especially Dr. Aslı Sade Memişoğlu, Müşerref Şeyma Ceyhan and Mümine Küçükdemir, who introduced me to the world of wet lab and endured my endless questions.

I would like to thank TÜBİTAK for the scholarship covering my expenses.

I would like to extend my thanks to Osman Karapür for his support, encouragement, and for keeping me sane since the primary school.

Many thanks to my parents Neşe and Hakkı Ünal Ülgen, and my brother Doruk Alp Ülgen for their understanding, encouragement, support, help and motivation.

Finally, I would like to express my gratitude and love to Melis Çolakoğlu; a recent lab mate, but an eternal soulmate.

TABLE OF CONTENTS

ABSTRACT.....	v
ÖZ	vii
ACKNOWLEDGEMENTS.....	x
TABLE OF CONTENTS.....	xi
LIST OF TABLES	xv
LIST OF FIGURES	xvi
CHAPTERS	
1. INTRODUCTION	1
1.1 Colorectal cancer.....	1
1.1.1 Caco-2 cell line	4
1.1.2 HT-29 cell line	4
1.2 Inflammation.....	5
1.2.1 Regulation of inflammatory genes.....	6
1.2.2 Chronic inflammation-cancer relationship.....	7
1.2.3 NF- κ B Pathway.....	8
1.2.4 Cyclooxygenase-2.....	11
1.3 mRNA stability of inflammatory genes.....	13
1.3.1 Involvement of p38 mitogen-activated protein kinase pathway in mRNA stability	14
1.3.2 HuR.....	16

1.3.3	TTP	17
1.4	Short-chain fatty acids	18
1.4.1	Sodium butyrate (NaBt): effects in normal cells and cancer cells 20	
1.4.2	Outcome of NaBt treatment: is it always working?	22
1.5	Aim of the Study	23
2.	MATERIALS AND METHODS	25
2.1	Cell culture	25
2.2	Treatments	25
2.3	RNA isolation and cDNA synthesis	27
2.4	RT-PCR and qRT-PCR	27
2.4.1	qRT-PCR for the usage of alternative polyadenylation signal ...	28
2.5	Analysis of protein expression	29
2.5.1	Total protein isolation	29
2.5.2	Cytoplasmic and nuclear protein isolation	30
2.5.3	Quantification of isolated proteins	30
2.5.4	Western blotting	30
2.6	Luciferase assay	32
2.7	Chromatin immunoprecipitation	33
2.8	Statistical analyses	34
3.	RESULTS	35
3.1	mRNA and protein levels of COX-2 upon NaBt treatment	35

3.2	Transcriptional regulation of COX-2 in the presence of NaBt	36
3.3	Post-transcriptional regulation of COX-2 in the presence of NaBt ...	41
3.3.1	Alternative polyadenylation of the 3'UTR of COX-2 mRNA....	41
3.3.2	p38-mediated post-transcriptional regulation of COX-2 mRNA	42
3.4	COX-2 mRNA stability increases upon NaBt treatment	45
3.5	HuR and TTP compete for COX-2 mRNA stability in NaBt-treated Caco-2 and HT-29 cells	48
4.	DISCUSSION	51
4.1	NaBt and inflammation.....	52
4.2	NF- κ B activity in the presence of NaBt.....	53
4.3	Post-transcriptional regulation of COX-2 mRNA	54
4.4	Differential activation of p38 MAPK in the presence of NaBt.....	56
4.5	Acquisition and loss of stability of COX-2 mRNA in Caco-2 and HT- 29 cells	57
4.6	p38 activation status as a prognostic marker for treatment with NaBt 60	
5.	CONCLUSION.....	61
6.	FUTURE STUDIES.....	63
	REFERENCES.....	65
	APPENDICES	
	Appendix A: Cytoplasmic HuR levels upon actinomycin D treatment	85
	Appendix B: Cloning of COX-2 3'UTR to the psiCheck2™ vector	89
	Appendix C: qRT-PCR standard curves	91

Appendix D: Minimum Information for Publication of Quantitative Real-Time PCR Experiments Guidelines	95
Appendix E: Contents of buffers used for Western Blot experiments	99
Appendix F: Maps of vectors used in this study	101

LIST OF TABLES

TABLES

Table 2.1: List of primers used in this study.....	29
Table 2.2: List of antibodies used in this study. Asterisk indicates the concentration used for chromatin immunoprecipitation.	31
Table D.1 The MIQE guidelines.....	96

LIST OF FIGURES

FIGURES

Figure 1.1 Progression of CRC; retrieved from (“From Polyp to Cancer” 2014).	2
Figure 1.2 Morphology of Caco-2 (A) and HT-29 (B) cells. Adapted from ATCC.....	5
Figure 1.3 Schematic representation of the two classes of NF-κB proteins. NF-κB (Class I) class contains a Rel-homology domain followed by several ankyrin repeats towards the N-terminus. Rel (Class II) class is equipped with a transactivation domain instead of the ankyrin repeats of Class I. Adapted from (Gilmore 2006).	9
Figure 1.4 COX-2 mRNA can be regulated by mRNA binding proteins CUGBP2 (A), HuR/TTP (B), miRNAs (C), and alternative polyadenylation (C, D). Adapted from (Harper and Tyson-Capper 2008).	12
Figure 1.5 The p38 MAPK pathway. Adapted from (Novus Biologicals 2014)	15
Figure 1.6 Chemical formula of NaBt. Taken from (Selleck Chem 2014).....	20
Figure 1.7 The range of effects of butyrate in normal versus CRC cells. Adapted from (Fung et al. 2012).....	21
Figure 2.1 Plan followed for the treatments. If the cells are to be treated with SB 202190 (SB), they are pre-treated with NaBt for 48 h. For actinomycin D experiments, all the cells (untreated, NaBt-treated, SB-	

treated, or SB+NaBt treated) were treated with actinomycin D after the time required for other treatments ended. Cells were then gathered at 0, 0.5, 1, 2, and 4 h-marks.....26

Figure 3.1 qRT-PCR analysis of COX-2 mRNA levels in untreated (UT) or with 48 h of treatment with 1, 3 and 5 mM NaBt in Caco-2 (A) and HT-29 (B). Data were normalized using β -actin levels. (C) Protein levels of COX-2 mRNA in the two cell lines treated with 3mM NaBt. β -actin was used as protein loading control.36

Figure 3.2 (A) Cytoplasmic-nuclear fractionation Western showing the changes in the subcellular localization of the NF- κ B subunits p65 and p50 in untreated (UT) or treated (NaBt) Caco-2 and HT-29 cells. Topoisomerase II- β (TopoII β) and α -tubulin were used as nucleus- and cytoplasm-specific markers, respectively; and β -actin was used as the loading control. Luciferase assay utilizing NF- κ B PathDetect plasmid in Caco-2 (B) and HT-29 (C).38

Figure 3.3 ChIP assay using antibodies of p65, p50, and IgG as negative control in Caco-2 (A) and HT-29 (B). After immunoprecipitating with the indicated antibodies, DNA fragments obtained were used as template in qRT-PCRs for COX-2 promoter region. Data was shown as fold enrichment with respect to IgG.40

Figure 3.4 qRT-PCR analysis of longer COX-2 transcript using primers against the site between the proximal and distal polyA signals. Significance calculated by comparing to the untreated sample. Data were normalized using β -actin levels.42

Figure 3.5 (A) Phospho-(Ty₁₈₂) and total p38 levels in cytoplasmic fractions of Caco-2 and HT-29 cell lysates. The upper band in p-p38 (marked with an asterisk) is non-specific. qRT-PCR for COX-2 mRNA in untreated, NaBt-treated, SB 202190-treated (SB) and Double-treated cells of Caco-

2 (B) and HT-29 (C). SB and Double samples were pre-treated with NaBt for 48 h. Asterisk indicates that after pre-treatment, the sample was treated with NaBt and SB together. Significance calculated by comparing to the untreated sample. Data were normalized using β -actin.45

Figure 3.6 Actinomycin D time course of untreated (blue), NaBt-treated (red), SB 202190-treated (green) and Double-treated (orange) Caco-2 cells. After the appropriate treatments, all cells were incubated with actinomycin D (1 μ g/ml) and harvested at the indicated time points. qRT-PCR data (A) were normalized using GAPDH as an internal control. In RT-PCR experiments (B), β -actin was used as loading control.46

Figure 3.7 Actinomycin D time course of untreated (blue) and NaBt-treated (red) HT-29 cells. After the appropriate treatments, all cells were incubated with actinomycin D (1 μ g/ml) and harvested at the indicated time points. qRT-PCR data (A) were normalized using GAPDH as an internal control. In RT-PCR experiments (B), β -actin was used as loading control.47

Figure 3.8 HuR levels in the cytoplasmic fraction from untreated or NaBt-treated Caco-2 and HT-29 cells (A). Total TTP levels from untreated or NaBt-treated Caco-2 and HT-29 lysates (B). β -actin was used as protein loading control.49

Figure 4.1 The schematic representation of COX-2 3'UTR, with the polyA signals and the AREs shown. The usage of the distal polyA signal generates a transcript that is 1.8 kb longer containing an additional 23 AREs. Adapted from (Hall-Pogar et al. 2005).....55

Figure A.1 Cytoplasmic HuR levels in Caco-2 and HT-29 cells treated with 1 μ g/ml for 30 min. Note that even though the exposure is quite lower as

compared to that in Figure 3.8, actinomycin D-induced levels of cytoplasmic HuR are clearly visible.	85
Figure A.2 Results of two representative actinomycin D time course experiments in Caco-2 (A) and HT-29 (B) cells.....	87
Figure C.1 Standard and melt curves used for COX-2 qRT-PCR primers.	92
Figure C.2 Standard and melt curves used for β -actin qRT-PCR primers.....	93
Figure C.3 Standard and melt curves used for GAPDH qRT-PCR primers...	94
Figure F.1 The base map for PathDetect cis-Reporter plasmids (Agilent Technologies). The NF- κ B PathDetect plasmid used in this study possesses five tandem repeats of the NF- κ B response element (TGGGGACCTTTCCGC).	101
Figure F.2 pSV- β -Galactosidase (Promega).	102
Figure F.3 psiCHECK TM -2 (Promega).	103

CHAPTER 1

INTRODUCTION

1.1 Colorectal cancer

Colorectal cancer (CRC), described as the cancer of the colon or rectum, is the third leading cause of cancer-related deaths in the United States regardless of gender, preceded only by lung cancer in both genders; prostate cancer in males and breast cancer in females (Siegel, Naishadham, and Jemal 2013; American Cancer Society 2014). CRC is highly prevalent, with a 5% risk of developing worldwide. Although there is a degree of inheritance associated with CRC, many of the risk factors are lifestyle-related. Diets low in fiber-containing fruits, vegetables, and high in over-cooked meats are linked to high risk of developing CRC. Thus, it has been recognized that, being a cancer of the gastrointestinal tract, CRC is extensively associated with the food metabolism of the body and that fiber-rich food has a protective effect (Bultman 2014).

CRC has an established model of progression and mutations. Fodde et al. suggested that in order to develop into cancer, an intestinal cell must first acquire the selective advantage to allow for the initial clonal expansion and the genetic instability to either abrogate the activity of tumor suppressors or reinforce genes responsible for malignant transformation (Fodde, Smits, and

Clevers 2001). From the normal mucosa to adenomatous polyps and then to adenomas (Figure 1.1), it was proposed that the cells should inactivate tumor suppressor proteins such as APC and p53; and activate transcription factors such as NF- κ B (described in section 1.2.2), AP-1, K-Ras, and SMAD4 (Brosens et al. 2005). Originating from a tissue that has a high turnover rate, it is hardly surprising that CRC also possesses a high mutation rate (Greenman et al. 2007).

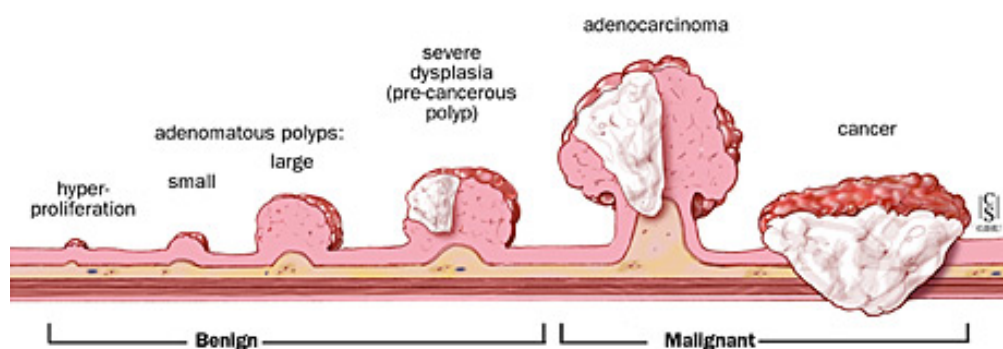


Figure 1.1 Progression of CRC; retrieved from (“From Polyp to Cancer” 2014).

When considering colorectal cancer progression, it is important to bear in mind that the colon is not a sterile environment; it is home to an array of bacterial strains that collectively constitute the microbiota. Commensal microbiota contributes to the health of colon through many processes

including the production of short-chain fatty acids such as acetate, propionate, and butyrate (please see section 1.4). The presence of bacteria leads to an induction of T- and B-cells of the immune system; however, this activation of the immune system is regarded as limited, and the colon is thought to be in a state of controlled inflammation where the commensal bacteria are tolerated (Cebra 1999). Moreover, a strong barrier function in the intestine keeps the bacterial population separate from the stroma. As will be discussed in section 1.2.2, a constant, low-level inflammation that does not resolve in the event of a breach in the barrier function might result in tissue damage that in turn leads to CRC transformation (Scanlan et al. 2008). Therefore, the regulation of immune response to the microbiota plays a key role in the homeostasis of the colon, and evidence suggests that such regulation can be exerted by the cross-talk of different strains of bacteria. To illustrate, a study showed that when germ-free mice were inoculated with *Bifidobacterium adolescentis* or *Bacteroidetes thetaiotaomicron*, immune response was generated only to *B. thetaiotaomicron*; however, a co-inoculation of the two strains relieved this response against *B. thetaiotaomicron*, implying that presence of *B. adolescentis* adjusted the humoral immunity against another strain (Scharek et al. 2000). Consequently, the products of bacterial metabolism (short-chain fatty acids, reactive oxygen species, etc.), cross-talk between different strains, and the regulation of the immune response are means by which microbiota constitution might influence CRC transformation and progression (Hope et al. 2005). Despite the fact that every individual has a unique constitution of microbiota in their colon, the identity, number, and the percentile of the residents appear important for a healthy colon (Sears and Garrett 2014).

Having been studied for many years, a number of *in vitro* model cell lines are available for CRC. In this study, Caco-2 and HT-29 cell lines were used, both of which were isolated in 1977 (Fogh et al. 1977).

1.1.1 Caco-2 cell line

A human colon adenocarcinoma cell line, Caco-2 cells are less potent, invasive and metastatic. As is the case for most CRC cell lines, Caco-2 cells grow in monolayers *in vitro*. These cells show increased dependence on fetal bovine serum in the medium; requiring two-fold of the usual concentration, and can spontaneously differentiate to enterocyte-like cells showing cell polarity and expressing small intestinal hydrolase enzymes (Pinto et al. 1983). The cell line possesses a high level of heterogeneity in culture, which is visible through a microscope. Being a rather heterogeneous cell line, there is a possibility that different labs working on it may have different subpopulations of Caco-2 that dominated the culture in the earlier propagations, and this may lead to non-comparable results. Therefore, to generate more analogous results, efforts have been made to establish standard culture conditions and the number of passages (Sambuy et al. 2005).

1.1.2 HT-29 cell line

HT-29 cells were isolated from a 44 year-old Caucasian female with colorectal adenocarcinoma (American Tissue Culture Collection 2014). Compared to Caco-2, HT-29 is a more aggressive cell line with a lesser requirement for growth factors *in vitro*. Although there are subpopulations with higher metastatic potential, HT-29 cells, relative to the other CRC cell lines, are generally regarded as less metastatic (Haier, Nasralla, and Nicolson 1999). Unlike Caco-2 cells, HT-29 cells do not undergo enterocytic differentiation spontaneously; rather, a glucose-free medium is required to induce the process (Zweibaum et al. 1985). The morphologies of the Caco-2 and HT-29 cells can be seen in Figure 1.2.

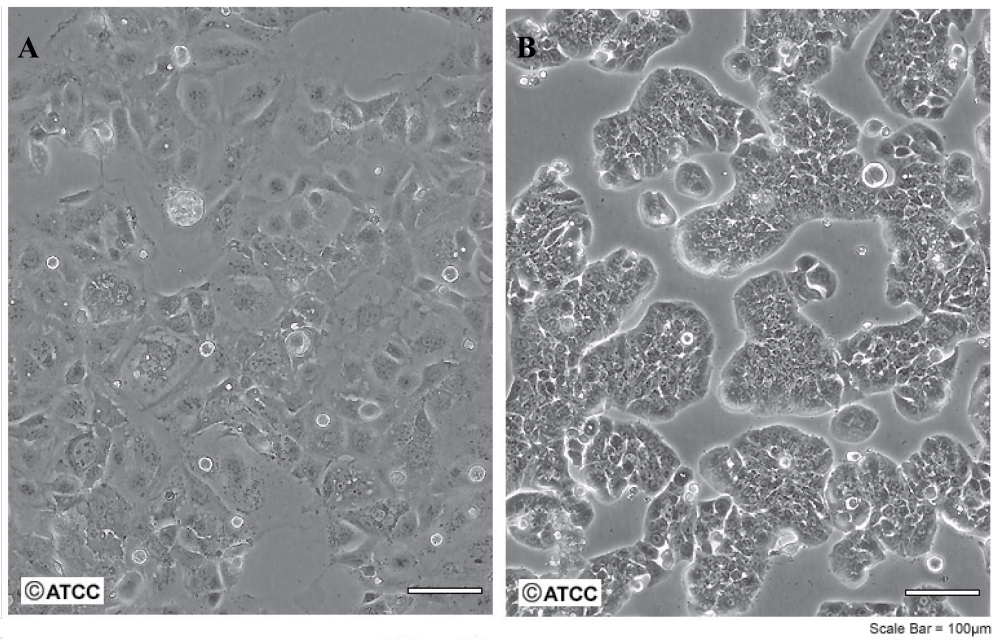


Figure 1.2 Morphology of Caco-2 (A) and HT-29 (B) cells. Adapted from ATCC.

1.2 Inflammation

A wound and the subsequent pathogen entry through the wound trigger a sophisticated network of molecular signaling within the body, whose ultimate purpose is to clear the pathogens at the site of infection (Medzhitov 2008). Its name comes from the “in-flamed” appearance of the site of injury due to an increase in the speed of the blood supply. Inflammation helps in the recruitment of leukocytes, cells of innate immune system specialized to exterminate pathogens, to the site of infection, guiding them by a gradient of chemokines. The leukocytes are then required to migrate out of the blood

vessel by a process known as extravasation (Middleton et al. 2002). Once the pathogenic threat is cleared by the leukocytes, inflammation recedes and with the aid of growth factors, epithelial cells are given clearance to migrate and proliferate to fill up the wound.

The proteins integral to the generation and sustainability of the inflammatory response are called pro-inflammatory proteins. Pro-inflammatory proteins can be exemplified by cytokines interleukin-1 β (IL-1 β), IL-6, TNF- α ; enzymes such as cyclooxygenase-2; and the transcription factors nuclear factor kappa B (NF- κ B, see section 1.2.3) and activator protein-1 (AP-1) (Adcock and Caramori 2001). The subsequent inactivation of inflammatory responses is regulated by anti-inflammatory proteins. Generally, anti-inflammatory proteins operate by counter-acting against the activity of pro-inflammatory proteins; and as a result, inflammation is resolved.

Healthy inflammation should progress acutely, dwindling as soon as the pathogen threat is removed (Buckley et al. 2013). The resolution of inflammation is required since prolonged inflammation interferes with wound healing. Furthermore, as will be described in section 1.2.2, a constant, low-level inflammatory environment is thought to promote neoplastic transformation (Coussens and Werb 2002). That inflammation can be rather destructive to the body itself necessitates extensive regulation of the genes involved in inflammatory response.

1.2.1 Regulation of inflammatory genes

Two master regulators of the inflammatory response are the transcription factors NF- κ B and AP-1, whose downstream target genes comprise a large group of pro-inflammatory genes (Wegener and Krappmann 2008; Karin, Liu, and Zandi 1997). However, the time required for the transcription of pro-inflammatory mRNAs and successive translation is rather long; and as stated

earlier, a more acute, rapid response is required for inflammation. Thus, many inflammatory genes are regulated not only at the transcriptional level but post-transcriptional, translational and post-translational level, as well (Bhatt and Ghosh 2014; Saccani, Pantano, and Natoli 2002; O'Connell, Rao, and Baltimore 2012). Post-transcriptional regulation provides rapid response owing to the lack of dependence on the production of new mRNA. Translational regulation ensures the fine-tuning of the inflammatory protein levels that rapidly increase when needed and diminish when not. Post-translational regulation supplies a second level of regulation over the activity of inflammatory proteins, so that they can be turned on or off swiftly.

1.2.2 Chronic inflammation-cancer relationship

The inflammatory environment presents a harsh living condition for the adjacent cells. Reactive oxygen and nitrogen species are utilized by leukocytes as a weapon against pathogens (Bryan et al. 2012). As described earlier, inflammation also involves anti-apoptotic signals, pioneered by NF- κ B, which provides survival signals to the surrounding tissue. On the other hand, if inflammation cannot be resolved and instead continues to exist at a low level (referred to as chronic inflammation), these mechanisms may also favor cancer progression and survival, respectively. Indeed, leukocytes had been observed within tumors by Rudolf Virchow in the 19th century. Since then, more and more evidence connects inflammation to cancer, with 20% of all cancer incidences attributed to chronic inflammation (Grivennikov, Greten, and Karin 2010). The relationship is much more prominent in the case of CRC, since 95% of CRC cases also show chronic inflammation (Siegel, Naishadham, and Jemal 2012). Keeping in mind the constant risk of microbiota in the colon running rogue and causing inflammation, these statistics are hardly surprising for CRC.

Whether inflammation precedes or succeeds tumor transformation or progression was initially a matter of debate; however, it is now understood that chronic inflammation might play a role in both of the cases. Before tumorigenic transformation, the required mutations are accelerated by genomic instability and epigenetic modifications exerted in the inflammatory milieu. Induction of growth factor-mediated tissue repair facilitates the proliferation of transformed cells; and the rapid proliferation, in turn, also contributes to the genomic instability. Upon passing the threshold up to which the blood supply can feed the early tumor, cells located inside the solid tumors undergo necrosis and the resulting release of IL-1 and high mobility group protein-1 (HMGB-1) ensures an angiogenic effect mediated by inflammation (Vakkila and Lotze 2004). The “wounds that do not heal” (Flier, Underhill, and Dvorak 1986), tumors both draw on and promote a low-level inflammation (Grivennikov, Greten, and Karin 2010).

1.2.3 NF- κ B Pathway

A potent activator of inflammatory responses, the NF- κ B family of proteins was first discovered in David Baltimore’s laboratory, and is characterized by its ability to bind immunoglobulin κ light chain enhancer sequences (Sen and Baltimore 1986). The family is divided into two classes with reference to the domains their proteins carry (Figure 1.3);

1. Class I contains NFKB1 and NFKB2 genes, which code for p105 and p102, respectively. After translation, these proteins undergo proteolytic cleavage to yield p50 and p52, which are the functional counterparts.
2. Class II is also known as the Rel-group of proteins due to the homology they share with the retroviral oncoprotein v-Rel; and although class I proteins also share this homology, class II took the name because its proteins were discovered earlier. This class is

comprised of RELA, RELB and c-Rel; RELA encodes the protein p65.

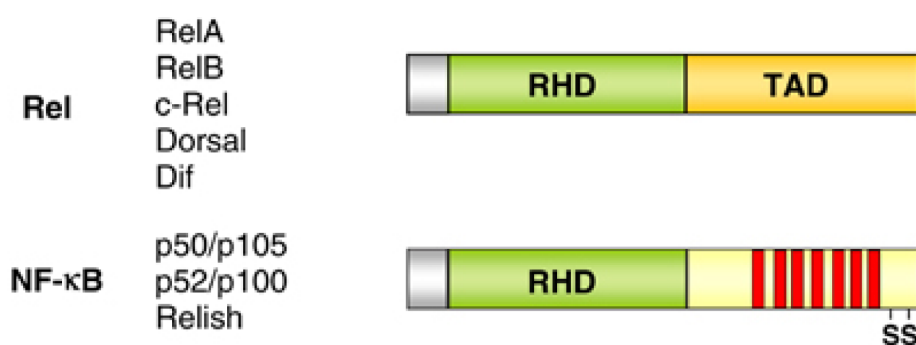


Figure 1.3 Schematic representation of the two classes of NF-κB proteins. NF-κB (Class I) class contains a Rel-homology domain followed by several ankyrin repeats towards the N-terminus. Rel (Class II) class is equipped with a transactivation domain instead of the ankyrin repeats of Class I. Adapted from (Gilmore 2006).

The proteins from both classes can either homodimerize or heterodimerize. Since they possess a transactivation domain, the homo- and heterodimers containing at least one subunit from Class II are assumed to have the ability to induce transcription; although this may not be true all the time (Paz-priel et al. 2013). Conversely, dimers of class I proteins are regarded as repressive due to the inability of ankyrin repeats to recruit proteins important in transcription initiation.

NF- κ B can bind DNA from the decameric sequence 5'-GGGRNWYYCC-3' where N is any nucleotide; W is A or T; and Y is C or T. Sequences on DNA conforming to the above formula are called NF- κ B-response elements and are usually found in the promoters of pro-inflammatory genes, as well as NF- κ B genes themselves.

The name NF- κ B usually refers to the canonical heterodimer of p65 and p50, and the heterodimer is sequestered in the cytoplasm by a family of proteins called inhibitor of κ -B (I κ B). Upon stimulation by pathogens, UV exposure or stress stimuli (Aggarwal 2004), I κ B α is phosphorylated by I κ B kinases (IKK) on serine residues 32 and 36, which renders the protein a target for ubiquitin-proteasome degradation system (Traenckner et al. 1995). Now free of the repression, NF- κ B translocates into nucleus, being able to induce transcription of NF- κ B-responsive inflammatory genes, as well as transcription of its own genes. Along with the genes responsible for the required physiological response, NF- κ B also increases the transcription of its repressor that is I κ B α , in the case of the canonical p65-p50 heterodimer, thereby ensuring that NF- κ B response is not preserved at the same level (Scott et al. 1993). While active, NF- κ B increases the transcription of cytokines and proteins involved in eicosanoid cascade such as 5-lipoxygenase and cyclooxygenase-2 (Pahl 1999).

Since the inflammatory environment can be severely damaging to the surrounding cells, NF- κ B also inhibits p53-mediated apoptosis and upregulates the transcription of several anti-apoptotic genes of the Bcl-2 family, promoting the survival of cells in the vicinity (Pahl 1999). These same pro-survival capabilities of NF- κ B confer a strong oncogenic role to the protein. Indeed, NF- κ B activity was observed to peak in many types of human cancers ranging from CRC to lymphomas (Staudt 2010).

1.2.4 Cyclooxygenase-2

Synthesized from the transcript of the gene prostaglandin-endoperoxidase synthase-2 (PTSG-2), cyclooxygenase-2 (COX-2) catalyzes the conversion of arachidonic acid to PGG₂; the key regulatory step in the anabolism of prostaglandins, most prominently PGE₂ (Park, Pillinger, and Abramson 2006). Despite catalyzing the same reaction with COX-1, unlike COX-1, COX-2 is not ubiquitously expressed; it is upregulated upon pathogen stimuli, nitric oxide, irradiation or cytokines, and once such signals cease, the levels of COX-2 are rapidly brought down (Harper and Tyson-Capper 2008). As described beforehand, COX-2 is among many inflammatory genes whose expression and activity are highly regulated both transcriptionally and post-transcriptionally and COX-2 mRNA is known to be regulated by microRNAs and mRNA binding proteins (see section 1.3) via its 3'-untranslated region (UTR). Furthermore, COX-2 transcript possesses two distinct polyadenylation signals, the utilization of which yield either a shorter 3'UTR containing relatively less regulatory sites; or a longer 3'UTR having more regulatory sites (Hall-Pogar et al. 2005) (Figure 1.4).

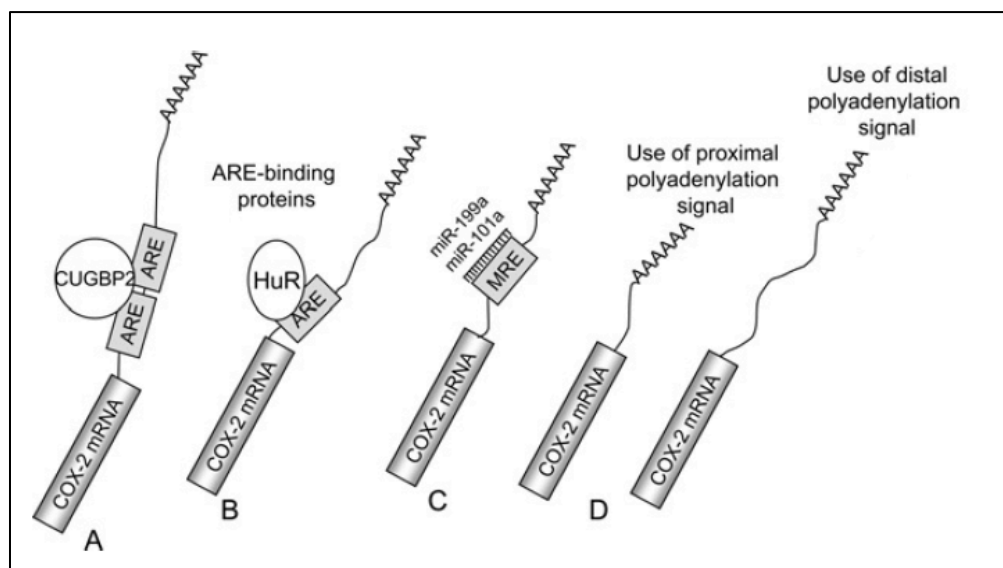


Figure 1.4 COX-2 mRNA can be regulated by mRNA binding proteins CUGBP2 (A), HuR/TTP (B), miRNAs (C), and alternative polyadenylation (C, D). Adapted from (Harper and Tyson-Capper 2008).

COX-2 mRNA levels and activity were observed to be increased in 85% of all CRC incidences (Eberhart et al. 1994). The first evidence that COX-2 activity was important in CRC came to light from a patient whose rectal polyps receded while he was prescribed a combination of indomethacin and sulindac for pain relief (Waddell and Loughry 1983). The studies that followed revealed that 10-15 years intake of the non-steroidal anti-inflammatory drug (NSAID) aspirin, which is an inhibitor of both COX-1 and COX-2, reduces the risk of developing CRC by up to 50% (Giovannucci et al. 1994; Ricchi et al. 2003). However, the clinically available COX-2 selective inhibitors celecoxib and rofecoxib have been shown to be more powerful chemotherapeutic agents than NSAIDs, suggesting that the inhibition of COX-2 could be the cause of NSAID-mediated cancer regression (Roelofs et

al. 2014). In a study using transgenic mice, it was demonstrated that overexpression of COX-2 alone could induce tumorigenesis (Liu et al. 2001). Overexpression of COX-2 also led to a marked elevation in the levels of BCL-2 in rat intestinal epithelial cells; and matrix metalloproteinases, whose expression is usually linked to an elevation in cell migration and invasion (Tsuji and DuBois 1995; Tsujii, Kawano, and DuBois 1997).

1.3 mRNA stability of inflammatory genes

mRNAs of many inflammatory genes, along with those of other genes that need a stringent translational control to regulate the protein activity, possess 3'UTR regulatory elements known as AU-rich elements (ARE). AREs are defined as 5'-AUUUA-3' motifs near U-rich regions in 3'UTRs and are known to recruit proteins collectively referred to as ARE-binding proteins (AREBP) (Malter 1989). AREBPs may act to confer either stability or instability to the mRNAs they bind to, depending on the identity of the protein. To illustrate, HuR increases the stability of its bound mRNA, whereas AUF1, TIA-1, TIAR, and Tristetraprolin (TTP) can render it vulnerable to deadenylation of the polyA tail by 3'-exonucleases and the subsequent degradation of mRNA (Beelman and Parker 1995). HuR and TTP are explored further in sections 1.3.2 and 1.3.3, respectively.

Some of the less-investigated proteins that were found to bind ARE probes in electrophoretic mobility shift assays include hnRNP A0-1, poly-A binding protein, glyceraldehyde-3-phosphate dehydrogenase, enoyl-CoA hydratase, heat shock proteins hsp70 and hsp110, and CUGBP2 (Dean et al. 2004). Whether these findings are relevant or just artifacts of *in vitro* studies remains to be assessed.

1.3.1 Involvement of p38 mitogen-activated protein kinase pathway in mRNA stability

The p38 group of mitogen-activated protein kinases (MAPK) was identified when it was found that upon stress or heat shock, a different signaling cascade involving a novel MAPK, p38, was getting activated (Rouse et al. 1994). Four isoforms have been acknowledged, two of which (α and β) are ubiquitously expressed, with the expression of the remaining two (γ and δ) being restricted to the brain. Heat, UV exposure, osmotic shock, inflammatory cytokines TNF- α and IL-1, and growth factor CSF-1 are all stimuli by which p38 can be turned on. Upon activation, p38 can phosphorylate MAPK-activated protein kinase-2 (MK2) and/or transcription factors such as p53 and C/EBP β . As a result of this plethora of downstream targets, p38 signaling may influence many cellular events ranging from development, differentiation, cell cycle, apoptosis and inflammation (Zarubin and Han 2005) (Figure 1.5).

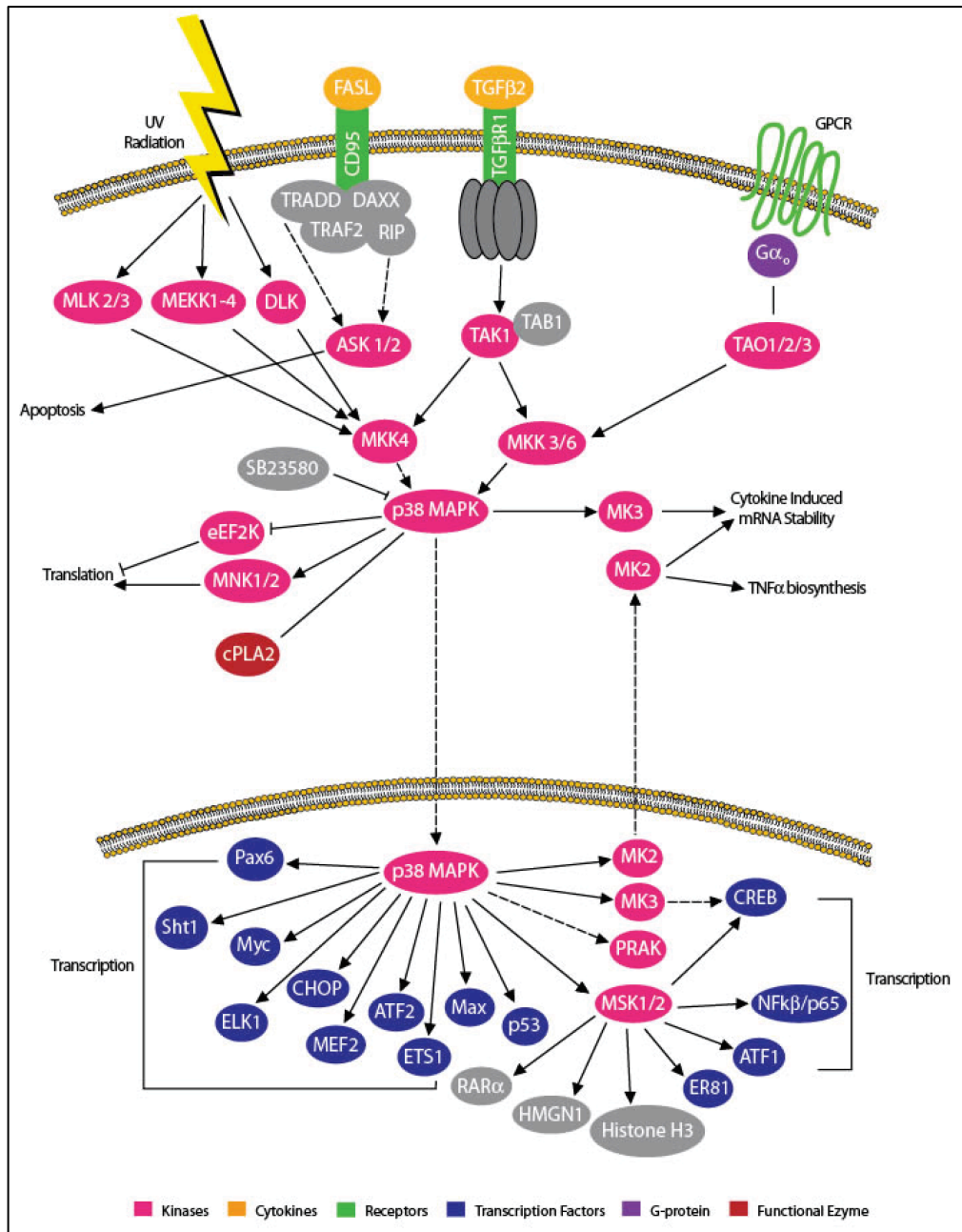


Figure 1.5 The p38 MAPK pathway. Adapted from (Novus Biologicals 2014)

p38 signaling is known to induce TNF- α and IL-1 production and COX-2 activity (W. Chen et al. 2001). It was later found that AREBPs HuR and TTP (see sections 1.3.2 and 1.3.3) are regulated by MK2, implying a role for p38 in mRNA stability of these proteins (F. Chen, Shyu, and Shneider 2011; Sawaoka et al. 2003). Indeed, TNF- α and COX-2 mRNAs have AREs in their 3'UTR (Espel 2005). p38 α/β inhibitors SB 203580 and SB 202190 were shown to inhibit inflammatory cytokine production, further corroborating that mRNA stability through p38 plays a considerable role in inflammatory responses (Badger et al. 1996).

1.3.2 HuR

Belonging to the family of embryonic lethal abnormal vision-like (ELAVL) proteins, HuR, or ELAVL1 is a crucial gene in the post-transcriptional regulation of ARE-containing mRNAs. The other members of the family, HuB, HuC and HuD have a brain-restricted tissue expression profile, whereas HuR is expressed in the intestine, thymus, spleen, and gonads (Lu and Schneider 2004). It is a 34 kDa protein that is predominantly localized in the nucleus (Xinhao Cynthia Fan and Steitz 1998). Upon p38-mediated activation of MK2, cyclin-dependent kinase-1 (Cdk1) is phosphorylated by MK2, which in turn phosphorylates HuR, promoting its translocation to the cytoplasm (Filippova et al. 2012). Now in cytoplasm, HuR can bind the AREs of mature transcripts and enhance their stability.

Overexpression of HuR in mouse NIH 3T3 cells was found to stabilize c-fos mRNA; however, this stability was not derived from the prevention of deadenylation of the polyA tail, as it was observed that there were deadenylated mRNAs in the stable mRNA pool (Peng et al. 1998). Likewise, an RNAi-utilized depletion of HuR resulted in a drop in mRNA levels of inflammatory cytokines, concurrent with a decline in protein levels. Another

intriguing finding was that muscle differentiation was severely inhibited upon HuR depletion (Van Der Giessen et al. 2003).

It is now an established notion that cytoplasmic HuR can stabilize ARE-containing mRNAs. Although the exact mechanism is still to be elucidated, shuttling of the protein between the nucleus and cytoplasm appears to be related to the hinge region between residues 205 and 237. It was reported that HuR, when methylated at its Arg²⁰⁶ or Arg²¹⁷ residues, can promote mRNA stability, implying that protein-protein interactions through the hinge region, and thus the shuttling and successive activity of the protein, can be modified (Li et al. 2002).

1.3.3 TTP

A protein with three tetraproline (PPPP) motifs, TTP is able to bind mRNAs at their 3'UTR AREs through two zinc-finger motifs (DuBois et al. 1990). It is a 36 kDa phosphoprotein whose expression is generally restricted to T lymphocytes, monocytes and macrophages (Ogawa et al. 2003). The deduction derived from the expression profile that TTP was important in innate immunity was substantiated when it was observed that TTP-null mice suffered from an inflammatory syndrome that arose from increased stability of TNF- α mRNA (Carballo, Gilkeson, and Blackshear 1997). Like HuR, TTP is also sequestered in nucleus, with a small fraction being in the cytoplasm. Upon direct phosphorylation by MK2 of the Ser⁵² and Ser¹⁷⁸ residues, nuclear TTP translocates into cytoplasm; however, unlike HuR, phosphorylated TTP loses its ability to bind AREs and instead are bound and kept in check by inhibitory 14-3-3 proteins (Chrestensen et al. 2004). One study revealed that degradation, but not the phosphorylation of the protein, is prevented by MG132, an inhibitor of 20S/26S proteasome, indicating phosphorylation of TTP does not precede ubiquitination and consequent degradation. The 14-3-3 binding kept TTP away from the stress granules and proteasomes, thereby

contributing to the stability, but not the activity of the protein (Brook et al. 2006). Hence, the p38-MK2 signaling improves mRNA stability by two separate means: by increasing the activity of stabilizing AREBP HuR, and by inhibiting the binding of destabilizing protein TTP to the AREs.

The seemingly counterintuitive effect of inflammatory p38 signaling over TTP; promoting the stability of the protein itself, is, in fact, another remarkable process by which pro-inflammatory signals are stringently regulated. It was proposed by Brook et al. that as soon as the inflammatory signals abate, mRNAs with AREs are actively destabilized by the now restored action of TTP (Brook et al. 2006). Since TTP is already at the location where it is functional, i.e., the cytoplasm, inflammation is resolved rapidly, without the need to anticipate the translocation of TTP.

HuR and TTP can regulate COX-2 mRNA stability through a number of AREs present in its 3'UTR. In the progression of CRC, it was observed that HuR activity was elevated, whereas TTP activity subsided; these phenomena were concurrent with the elevation of COX-2 mRNA levels (D. A. Dixon et al. 2001; L. E. Y. and D. A. Dixon 2010). However, despite its strong correlation with CRC, constitutive activity of p38 does not always occur in all cancer types, indicating that other signaling mechanisms are also in place to regulate the stability of the COX-2 mRNA (Comes et al. 2007).

1.4 Short-chain fatty acids

Compounds with fatty acid tails having less than six carbons are defined as short-chain fatty acids (SCFAs) (Cummings 1981). The most prominent members include acetic acid, propionic acid, and butyric acid; and their conjugate bases, acetate, propionate, and butyrate respectively, which are the compounds present in the body (Topping and Clifton 2001). SCFAs are

produced by the commensal microbiota present in the colon, through the fermentation of dietary fibers (Fung et al. 2012). There have been studies where SCFA production from mammalian tissues is implicated, however, the majority of the SCFAs are still derived from fiber fermentation. As a result, diet and microbiota composition of the individuals significantly influence the production of SCFAs.

The otherwise unavailable source of carbon-derived energy in fibers can be harvested in the body via β -oxidation of SCFAs. Depending on the production levels, 5-15% of the caloric requirement of the whole body can be contributed by SCFAs. The contribution of SCFAs to the mammalian energy requirement is the highest in the colon, as colonocytes preferably use butyrate over glucose and other fatty acids as an energy source. Liver and muscle cells can also utilize butyrate to obtain energy, but this is less favored (Velázquez, Lederer, and Rombeau 1997).

All SCFAs can be absorbed actively through their respective carrier proteins on the apical membrane, or passively through diffusion. The transport is highest in the ascending colon, where the SCFA concentration is reported to be in the range of 13-130 mM (Cummings et al. 1987). Among the SCFAs, acetate is predominant, and butyrate is the lowest. The bulk of the absorbed butyrate is used by the colonic epithelium, which results in yet lower portal levels, and the remaining levels are brought down even more by the liver. The venous concentration of butyrate is thus the lowest, as compared to the other SCFAs, ranging from 0.5 μ M to 3.3 μ M, while acetate, for example, has a serum concentration of 98-143 μ M (Wolever et al. 1997).

Despite acetate being the most prominent, butyrate has been studied the most extensively due to its potential anti-tumorigenic effects.

1.4.1 Sodium butyrate (NaBt): effects in normal cells and cancer cells

The sodium salt of butyrate, NaBt is an SCFA consisting of a four carbon-long fatty acid chain (Figure 1.6). In the colon, 60% of the mucin-adhered microbiota belongs to the Clostridium cluster XIVa, whose members are responsible for the production of virtually all the butyrate present in the colon (Van den Abbeele et al. 2013).

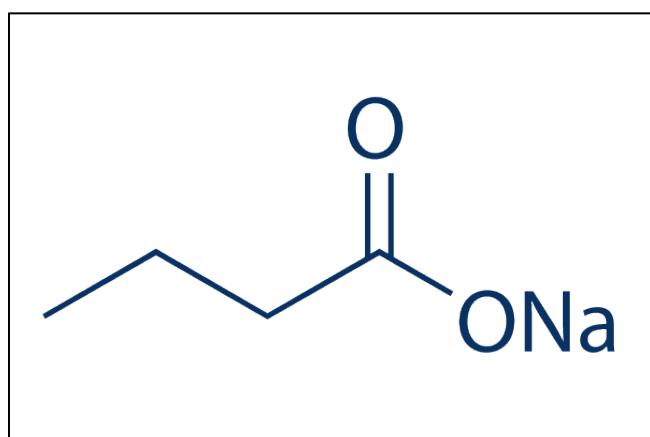


Figure 1.6 Chemical formula of NaBt. Taken from (Selleck Chem 2014).

Produced from bacterial fermentation, butyrate is used as the primary energy source by the colonocytes, another indication of the co-evolution humans went through with the microbiota (Donohoe et al. 2011). However, this is not the only physiological function of butyrate. The fatty acid is also crucial in colonic homeostasis, as it promotes the integrity of the mucosal barrier;

modulates immune and inflammatory responses; moderates fluid and electrolyte flux; regulates colonic motility, cell growth and differentiation (Figure 1.7). In the case of tumorigenic transformation, NaBt takes up new roles, presumably due to the shift of energy metabolism in cancer cells. Due to the Warburg effect, glucose is selectively used to obtain energy, which results in accumulated concentrations of NaBt in the cell (Donohoe et al. 2012). The lower extent of NaBt metabolism in turn yields the new roles such as induction of apoptosis and differentiation; inhibition of proliferation, cell cycle, angiogenesis and histone deacetylase (HDAC) activity (Candido, Reeves, and Davie 1978).

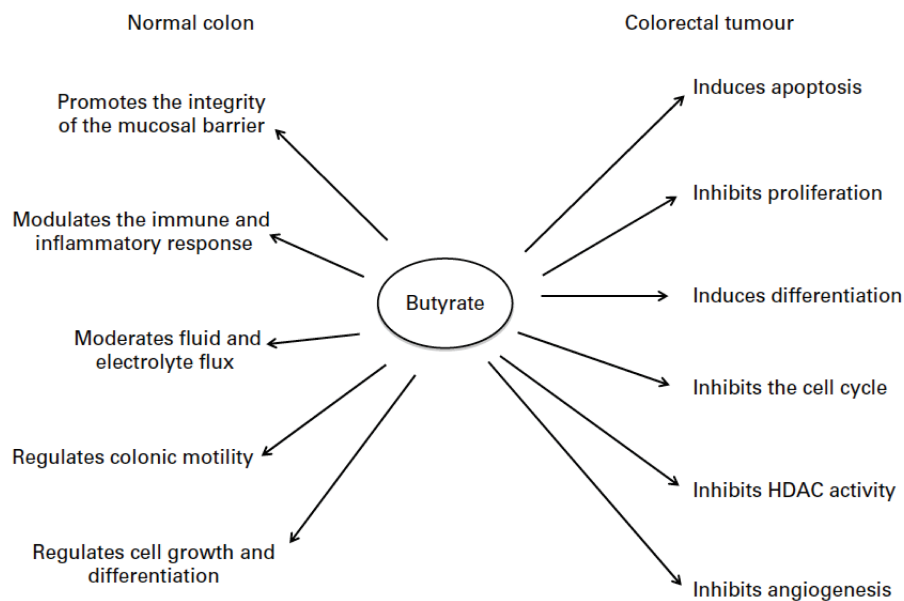


Figure 1.7 The range of effects of butyrate in normal versus CRC cells. Adapted from (Fung et al. 2012).

Among the tumor-induced effects of NaBt, HDAC inhibition is the most studied. Acetylated histones correspond to a more relaxed chromatin topography that is more accommodating to the transcription initiation complex; therefore, prevention of deacetylation by NaBt leads to a global increase in transcription; some direct targets being the Cdk inhibitor p21 and pro-apoptotic genes such as BAX and FAS (H M Hamer et al. 2008). NaBt can also modulate colonocyte differentiation through the regulation of genes such as mucins and intestinal alkaline phosphatases (Gum et al. 1987).

Chronic inflammation was also suggested to be relieved to an extent by NaBt, through a reduction in the expression of IL-8 and inhibition of nitric oxide synthase (Huang et al. 1997). Acetylated p65 subunits of NF- κ B are proposed to be more prone to I κ B-mediated inhibition, and since there is evidence suggesting that deacetylase-inhibitory effects of NaBt might not be confined to HDACs only, it is reasonable to assume that NF- κ B activity is also modulated by NaBt (Kiernan et al. 2003). Aside from these, NaBt was also found to inhibit transcription of c-myc and HIF-1 α , thereby inhibiting important promoters of tumorigenesis and angiogenesis, respectively (Heruth et al. 1993; Zgouras et al. 2003). These effects collectively reduce the survivability and the proliferation of cancer cells; and today, NaBt is being used as adjuvant in CRC treatment (Food and Drug Administration 2015). Although there are numerous studies conducted on NaBt alleviating different types of cancer *in vitro*, probably only those involving CRC cell lines hold relevance, as NaBt has a rather low concentration in the blood stream and the only location where it has a physiologically relevant concentration is the colon (Bultman 2014).

1.4.2 Outcome of NaBt treatment: is it always working?

Being highly selective for cancer cells and having a wide variety of effects by which chronic inflammation can be relieved, NaBt holds promise as a

chemotherapeutic against cancer and inflammatory diseases. On the other hand, not all patients receiving NaBt appear to be responding to the treatment. To illustrate, one study revealed that patients with ulcerative colitis in remission do not gain significantly beneficial effects upon NaBt treatment (Henrike M. Hamer et al. 2010). Mariadason et al. revealed that spontaneously differentiating Caco-2 cells gradually become more resistant to NaBt, postulating that this may have resulted from the increased metabolism of NaBt in the differentiated cells (Mariadason et al. 2001). It appears that availability of other inter-/intracellular factors and substrates, inflammatory conditions in the environment, differentiation status of the cell, and the constitution of microbiota influence the outcome of the treatment and whether a patient will benefit from it. Although there is no reported case of NaBt exacerbating the disease, the aforementioned ambiguity raises questions regarding NaBt's use as a chemotherapeutic drug.

1.5 Aim of the Study

Understanding the subtle molecular differences between CRC cell lines upon NaBt treatment is important to reveal as to why some patients do not benefit from NaBt use. Focusing on inflammation;

- We observed a differential regulation of the mRNA and protein levels of the highly inflammatory gene COX-2 upon NaBt treatment in two CRC cell lines; Caco-2 and HT-29.
- We then set out to investigate what this regulation entails and found that post-transcriptional, rather than transcriptional, regulation was more determining.

- The post-transcriptional regulation was conferred by the activation of p38 pathway in Caco-2 cells, which was lacking in NaBt-treated HT-29 cells.

This study illustrates that NaBt, though an HDACi, can also influence p38-driven mRNA stability of COX-2, which in turn leads to an increase in the protein levels.

CHAPTER 2

MATERIALS AND METHODS

2.1 Cell culture

Caco-2 and HT-29 cells were purchased from ŞAP Enstitüsü (Ankara, Turkey). Caco-2 cells were grown in Eagle's minimum essential medium (EMEM) (Biochrom AG, Germany) supplemented with 1% penicillin-streptomycin, 2 mM L-glutamine, 1.5 g/L sodium bicarbonate, 0.1 mM non-essential amino acids, 1 mM sodium pyruvate, and 20% fetal bovine serum (FBS). HT-29 cells were grown in McCoy's 5A medium (Biochrom AG, Germany), with 1% penicillin-streptomycin, 2 mM L-glutamine, and 10% FBS. Both cell lines were incubated at 37 °C, with 5% CO₂.

2.2 Treatments

Sodium butyrate (Sigma-Aldrich, Germany) was prepared fresh as a stock solution of 100 mM in cell culture-grade PBS, kept at -20 °C, and utilized in the treatments of 48 h with concentrations ranging between 1-5 mM in complete media. To prevent oxidation, the aliquots were stored under argon.

SB 202190 (Tocris Bioscience, United Kingdom) was prepared as a 100 mM stock in DMSO and stored in aliquots to avoid freeze-thaw cycles. Before use, the stock was further diluted to 10 mM, and the treatments, at a final concentration of 10 μ M, were done in serum-free media for 30 min.

Actinomycin D (Tocris Bioscience, United Kingdom) was prepared as 1 mg/ml stocks and aliquots were stored at -20 °C. Treatments were done in serum-free media after the pre-treatments with the appropriate chemicals, at the final concentration of 1 μ g/ml for 30 min.

The scheme for the treatments can be found in Figure 2.1.

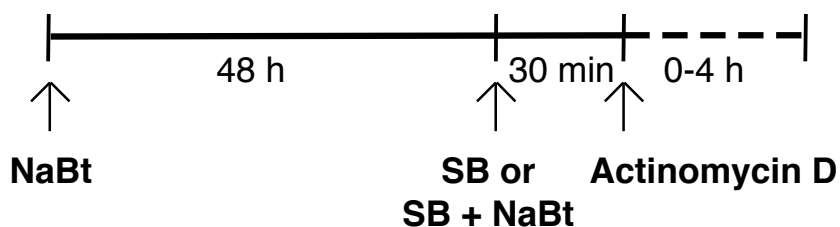


Figure 2.1 Plan followed for the treatments. If the cells are to be treated with SB 202190 (SB), they are pre-treated with NaBt for 48 h. For actinomycin D experiments, all the cells (untreated, NaBt-treated, SB-treated, or SB+NaBt treated) were treated with actinomycin D after the time required for other treatments ended. Cells were then gathered at 0, 0.5, 1, 2, and 4 h-marks.

2.3 RNA isolation and cDNA synthesis

After the appropriate treatments of sodium butyrate (48 h), SB 202190 (30 min) and/or actinomycin D (30 min), cells were gathered in cell culture-grade PBS, and total RNA isolation was carried out using RNeasy RNA Extraction Kit (Qiagen, Germany) according to the manufacturer's guidelines. To remove any contaminating genomic DNA, the RNA was treated with DNase I (Thermo Scientific, USA) and cDNA synthesis was carried out with 1 µg of the RNA with the RevertAid First Strand cDNA Synthesis Kit (Thermo Scientific) using oligo-dT primers (supplied in the same kit). The cDNAs were stored at -20 °C.

2.4 RT-PCR and qRT-PCR

RT-PCR mixtures were prepared in a volume of 18 µl with 0.5 µM forward and reverse primers (Table 2.1), 0.2 mM dNTP mix, 1.5 mM MgCl₂, and 1 U Taq Polymerase (Fermentas, Lithuania), into which 2 µl of 1 µg cDNA (final concentration: 0.1 µg) was added. Initial denaturation (3 min) and denaturation (30 sec) steps were carried out at 94-95 °C, and extension (30 sec) and final extension (7 min) steps were done at 72 °C, with the annealing temperatures and cycle numbers indicated in Table 2.1. The reactions were performed in a thermal cycler (Applied Biosystems). As an internal control, primers amplifying either GAPDH or β-actin were used. If the annealing temperatures of the primer sets of the gene of interest and the internal control were compatible, duplex PCR was utilized; if not, separate reactions were prepared for the primer sets. 20 µl of PCR product was mixed with 4 µl of 6X loading dye and run on a 2% agarose gel at 100V; images were observed and recorded under UV light.

For qRT-PCR, 18 μ l reactions were prepared with 0.5 μ M forward and reverse primers and 10 μ l of 2X Fast Start SYBR Green Mix, into which 2 μ l cDNA (final concentration: 0.01 μ g) was added. Either β -actin or GAPDH amplifications were used as internal controls. Reactions were carried out in Rotor GeneQ 6000 (Qiagen). Standard curves were prepared for each set of primers used, which were then used to calculate Ct values of the unknown samples. Fold changes with respect to the internal controls were calculated using Pfaffl method (Pfaffl 2001).

2.4.1 qRT-PCR for the usage of alternative polyadenylation signal

Primer sets against a sequence before the proximal polyA signal (named “shorter 3’UTR” in Table 2.1) and in between the proximal and distal polyA signals (named “longer 3’UTR” in Table 2.1) were constructed. qRT-PCRs were performed as described in section 1.4. The values obtained from shorter 3’UTR reaction were normalized by subtracting the longer 3’UTR values.

Table 2.1: List of primers used in this study

Description	Sequence	Annealing		Amplicon Length (bp)
		Temp. (°C)/	Cycle Number	
COX-2 (gene)	5'-CAAATCCTTGCTGTTCCCACCCAT-3'	65	40	173
	5'-GTGCACTGTGTTTGGAGTGGGTTT-3'			
COX-2 (promoter)	5'-CAAGGCGATCAGTCCAGAAC-3'	62	40	465
	5'-GGTAGGCTTTGCTGTCTGAG-3'			
COX-2 (longer 3'UTR)	5'-TCAGCTCAGGACTGCTATTTAG-3'	60	40	151
	5'-TTTGCATCCATCTTGGTTACAG-3'			
COX-2 (shorter 3'UTR)	5'-TTGCGGAGAAAGGAGTCATAC-3'	59,5	40	216
	5'-CAGCATTTTGCCATCTTGTG-3'			
GAPDH #1	5'-CGACCACTTTGTCAAGCTCA-3'	65	35	238
	5'-CCCCTCTTCAAGGGGTCTAC-3'			
GAPDH #2	5'-GGTGAAGGTCGGAGTCAACG-3'	57	35	497
	5'-CAAAGTTGTCATGGATGACC-3'			
β-actin	5'-CAGCCATGTACGTTGCTATCCAGG-3'	60,5	35	151
	5'-AGGTCCAGACGCAGGATGGCATG-3'			

2.5 Analysis of protein expression

2.5.1 Total protein isolation

M-PER Mammalian Protein Extraction Kit (Thermo Scientific) was used to extract proteins from cells, along with the additional protease and phosphatase inhibitors (Roche, Germany), and 0.2% NP-40 (Applichem).

2.5.2 Cytoplasmic and nuclear protein isolation

Cells ($\sim 10^7$) were gathered, and washed with cell culture-grade PBS containing phosphatase inhibitor twice, and resuspended in 500 μ l of hypotonic buffer (10 mM HEPES pH 7.5, 4 mM sodium fluoride, 10 μ M sodium molybdate, 0.1 mM EDTA, phosphatase and protease inhibitors). After 15 min incubation on ice, 100 μ l of 10% NP-40 was added and mixed by pipetting. Centrifugation at the highest setting for 30 sec yielded the supernatant that contained the cytoplasmic fraction. After the separation of cytoplasmic fraction into an ice-cold 1.5-ml tube, the pellet was resuspended in 100 μ l nuclear extraction buffer (10 mM HEPES pH 7.9, 0.1 mM EDTA, 1.5 mM $MgCl_2$, 420 mM NaCl, 20% glycerol, 1 mM dithioereitol, phosphatase and protease inhibitors). Samples were incubated on ice for 15 min, and vortexed at the highest setting, followed by another 15 min incubation on ice and another vortexing for 30 sec. Samples were then centrifuged down at 14000 g for 10 min at 4 °C. Supernatant, which contained the nuclear fraction was taken into another ice-cold 1.5 ml-tube. Cytoplasmic and nuclear fractions were stored at -80 °C.

2.5.3 Quantification of isolated proteins

Measurements for the isolated proteins were done using Coomassie Protein Assay Reagent (Thermo Scientific), relative to the bovine serum albumin standard curve.

2.5.4 Western blotting

Electrophoresis were carried out on a 10-12% SDS-polyacrylamide gel loaded with equal amounts of protein (30-70 μ M) at 100V. Wet transfer was performed to blot the proteins onto polyvinylidene fluoride membranes

(Roche), with constant current at 380 mA for 1 h and 15 min. The membranes were blocked in either 5% skim milk (Applichem) in PBS containing 0.1% Tween (Applichem) or 5% BSA (Applichem) in TBS containing 0.1% Tween, for 45 min at room temperature on a shaker. Overnight incubation with the primary antibody (Table 2.2) at 4 °C was followed by horseradish peroxidase-conjugated secondary antibody incubation for 1 h at room temperature, on the shaker. Visualization was performed using either Pierce ECL Western Blotting Substrate (Thermo Scientific) or Clarity ECL Substrate (Bio-Rad, USA) and imaged on a Chemi-Doc MP (Bio-Rad).

Table 2.2: List of antibodies used in this study. Asterisk indicates the concentration used for chromatin immunoprecipitation.

Description	Origin	Vendor	Media	Dilution	Conc. for ChIP (μg)
β -actin	mouse	Santa Cruz Biotech.	PBS-T	1:2000	-
α -tubulin	mouse	Santa Cruz Biotech.	PBS-T	1:500	-
Topoisomerase II β	rabbit	Santa Cruz Biotech.	PBS-T	1:500	-
p65	rabbit	Santa Cruz Biotech.	PBS-T	1:500	2.5
p50	rabbit	Santa Cruz Biotech.	PBS-T	1:500	2.5
p38	rabbit	Abcam	PBS-T	1:500	-
phospho-p38	rabbit	Santa Cruz Biotech.	TBS-T	1:500	-
HuR	rabbit	Abcam	TBS-T	1:1000	-
TTP	rabbit	Abcam	PBS-T	1:500	-
IgG	rabbit	Santa Cruz Biotech.	-	1:2000	2.5
anti-rabbit	goat	Santa Cruz Biotech.	PBS-T	1:2000	-
anti-mouse	rabbit	Santa Cruz Biotech.	PBS-T	1:2000	-

2.6 Luciferase assay

NF- κ B activity was assessed using pNF- κ B Luc PathDetect plasmid (Agilent) and pSV- β -galactosidase control vector was used as an internal control (Promega, USA). Caco-2 and HT-29 cells were transfected with 1 μ g/well of both vectors with X-tremeGENE HP (Roche) using a 1:3 μ g vector/ μ l transfection reagent ratio. Opti-MEM (Gibco, New Zealand) was used as the transfection medium. After incubating for 6 h at 37°C, transfection media were replaced with either EMEM or McCoy's 5A complete medium, in which sodium butyrate treatment was carried out for 48 h. Cells were harvested with 100 μ l lysis buffer (Roche) and cell debris were pelleted by centrifugation at 14000 x g for 2 min. The supernatant was transferred into a separate tube and 20 μ l was further aliquoted for luciferase measurements. The aliquots were mixed with 100 μ l luciferase assay reagent (Roche) and the Modulus Luminometer (Turner Biosystems, USA) was used to measure the relative light units at ~562 nm. In a separate 96-well plate, 50 μ l of supernatant was mixed with 50 μ l β -gal reaction buffer containing 100 mM β -mercaptoethanol (Sigma), 2 mM MgCl₂ (AppliChem), 200 mM sodium phosphate (Sigma) and 2-nitrophenyl β -D-galactopyranoside (Fluka, Germany). After 30 min incubation at 37 °C, absorbance values were measured by MultiSkan GO Microplate Spectrophotometer (Thermo Scientific).

For the 3'UTR luciferase experiments, Dual-Glo Luciferase Assay Kit (Promega) was used. 3'UTR of PTGS-2 gene were ligated into a psiCheck2 (Promega) vector (please see Appendix B). Cells were washed and harvested in 100 μ l Dual-Glo luciferase reagent for 15 min on a shaker at room temperature. Cells were gathered, and 20 μ l of lysate was transferred into white 96-wells and luminescence from firefly luciferase was measured by luminometer (Turner Biosystems, USA) after incubation with 25 μ l of

Luciferase Assay Reagent II (LAR II). Renilla luciferase activity was then measured immediately after incubation with 25 μ l Stop&Glo Reagent.

2.7 Chromatin immunoprecipitation

Cells were grown in 10-cm dishes. After the appropriate treatments, 0.8% formaldehyde was used to crosslink DNA-protein complexes. After incubating for 7 min, 125 mM glycine was added to stop the crosslinking reaction. Two washing steps were carried out with PBS, after which the cells were gathered in ice-cold PBS, into 1.5-ml eppendorf tubes. Centrifugation at 13000 x g for 1 min at 4 °C yielded the DNA-protein complexes as the pellet. The supernatant was discarded, and pellets were snap-frozen in liquid nitrogen. Buffer A containing 200 M HEPES-KOH pH 7.5, 420 mM NaCl, 0.2 mM EDTA pH 8.0, 1.5 mM MgCl₂, 25% glycerol and protease inhibitors was used to dissolve the pellet and incubated for 20 min on ice. After centrifugation to pellet the nuclei, the supernatant was discarded and the pellet was resuspended in Buffer B (50 mM Tris-Cl pH8.0, 1 mM EDTA, 1% SDS, 150 mM NaCl, 2% Triton X-100). A probe sonicator was used to shear DNA to lengths between 200-1000 bp. The sonication was pre-optimized and involved 11 cycles of sonication for 30s and incubation on ice for 30 sec each. An aliquot of 75 μ l was taken from the sheared chromatin, and de-crosslinking was carried out by incubating the chromatin with RNase A for 1 h (37 °C) and proteinase K (50 °C) for 1 h. The mixture was then incubated overnight at 60 °C after diluting it in 325 μ l of Buffer C (50 mM Tris-CL pH 8.0, 1 mM EDTA, 150 mM NaCl, 0.1% Triton X-100). Sheared chromatin amount was measured from the de-crosslinked input sample using NanoDrop (Thermo Scientific), and was run on a 1% agarose gel to confirm the efficiency of sonication. If the sheared DNA was of the required length, samples were divided into fresh 1.5 ml-eppendorf tubes so that each tube

contained 25 µg chromatin. The tubes were centrifuged at 13000 rpm for 10 min at 4 °C and the pellet was resuspended in Buffer C. Protein A/G beads (Santa Cruz) were pre-blocked with 1.5 µl of 1 µg/µl calf thymus DNA and 7.5 µl of 10 mg/ml BSA for 30 min on a shaker. Resuspended samples were then incubated in 2.5 µg of p65, p50 or isotype-specific IgG antibodies (Table 2) overnight at 4 °C with constant shaking. Pre-blocked beads were added onto the samples and incubated for 2 h at 4 °C on a shaker and samples were washed with Buffer 1 (20 mM Tris-Cl pH 8.0, 150 mM NaCl, 2 mM EDTA, 0.1% SDS, 1% Triton X-100) three times and then with Buffer 2 (20 mM Tris-Cl pH 8.0, 500 mM NaCl, 2 mM EDTA, 0.1% SDS, 1% Triton X-100) once. Elution Buffer (100 mM NaHCO₃, 1% SDS) was used to elute DNA-chromatin complexes, which were then subjected to the de-crosslinking procedure as input. Next day, DNA was obtained using HighPure PCR Purification Kit (Roche) and qRT-PCR experiments were performed to assess the quantity of the precipitated NF-κB response element-containing COX-2 promoter regions.

2.8 Statistical analyses

Experiments were repeated independently at least three times and Student's t-test or one-way ANOVA tests of GraphPad Prism 6.1 (GraphPad Software Inc., USA) were used to assess significance, with $p < 0.05$ considered to be significant.

CHAPTER 3

RESULTS

3.1 mRNA and protein levels of COX-2 upon NaBt treatment

Caco-2 and HT-29 cells were treated with physiologically relevant levels of NaBt (1-3 mM) and the adjuvant concentration (5 mM) for 48h and the expression of COX-2 was assessed. qRT-PCR analysis revealed that COX-2 mRNA levels were increased with NaBt treatment of Caco-2 cells, reaching their peak with 3 mM and declining from then on (Figure 3.1A). On the other hand, in HT-29 cells, COX-2 mRNA levels were decreased with the treatment, reaching the lowest levels with 3 mM NaBt (Figure 3.1B). The changes in the mRNA levels correlated with the COX-2 protein levels in the two cell lines (Figure 3.1C). Since the difference was the most pronounced at 3 mM, it was chosen as the treatment concentration for further experiments.

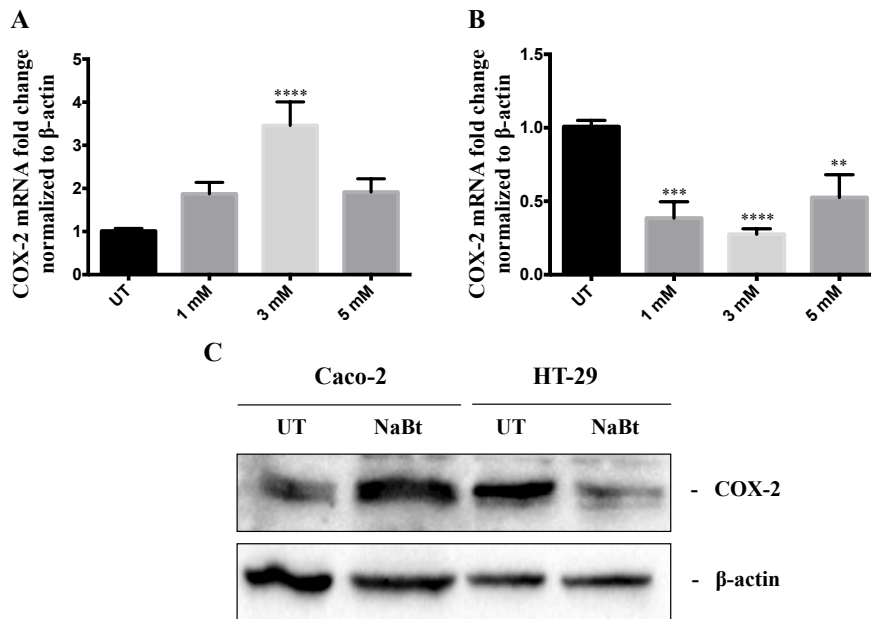


Figure 3.1 qRT-PCR analysis of COX-2 mRNA levels in untreated (UT) or with 48 h of treatment with 1, 3 and 5 mM NaBt in Caco-2 (A) and HT-29 (B). Data were normalized using β-actin levels. (C) Protein levels of COX-2 mRNA in the two cell lines treated with 3mM NaBt. β-actin was used as protein loading control.

3.2 Transcriptional regulation of COX-2 in the presence of NaBt

NF-κB is known to be one of the major regulators of COX-2 expression (Takada et al. 2004). Therefore, to investigate the underlying mechanisms of the differential regulation observed in the two cell lines, we first investigated the NF-κB activity. Nuclear/cytoplasmic fractionation showed that NaBt

treatment resulted in p65 translocation into the nucleus in Caco-2 cells, whereas in HT-29 p65 translocation showed little to no change. The overall p50 levels declined with NaBt treatment in both cell lines, with HT-29 demonstrating a more conspicuous change, especially in the nuclear fraction. Although α -tubulin used as the cytoplasmic marker was observed to be increased with treatment, β -actin levels demonstrated equal loading (Figure 3.2A).

To observe NF- κ B activity, we used the NF- κ B Pathdetect System®, a commercial luciferase plasmid containing five tandemly repeated NF- κ B-response elements upstream of the luciferase gene. After transfection and treatment with NaBt, luminescence levels normalized to β -galactosidase activity were expressed as fold change with respect to untreated samples. NF- κ B activity was found to be increased upon NaBt treatment in Caco-2, while HT-29 showed a decrease (Figure 3.2B-C).

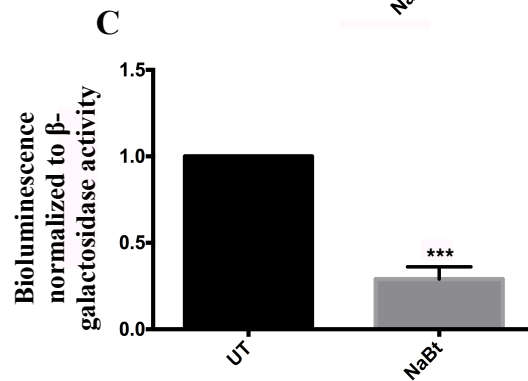
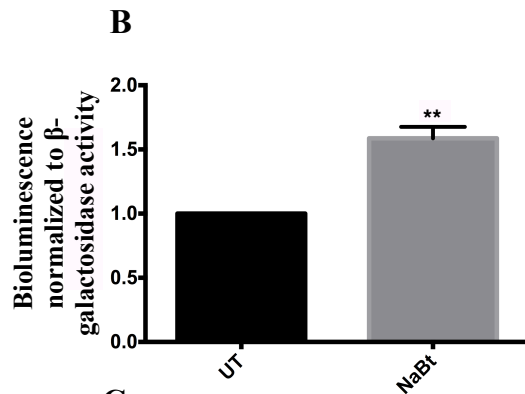
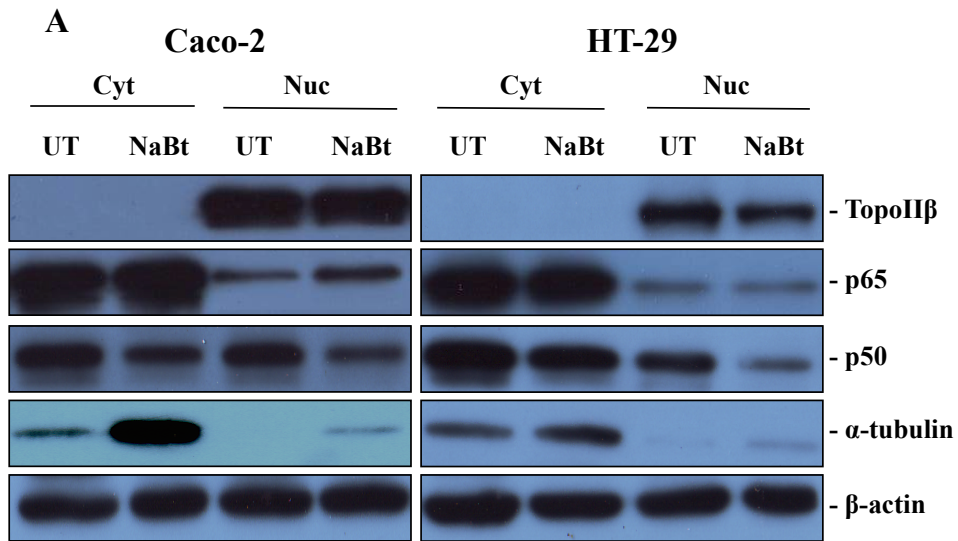


Figure 3.2 (A) Representative image of cytoplasmic-nuclear fractionation Western showing the changes in the subcellular localization of the NF-κB subunits p65 and p50 in untreated (UT) or treated (NaBt) Caco-2 and HT-29 cells. Topoisomerase II-β (TopoIIβ) and α-tubulin were used as nucleus- and

cytoplasm-specific markers, respectively; and β -actin was used as the loading control. Luciferase assay utilizing NF- κ B PathDetect® plasmid in Caco-2 (B) and HT-29 (C).

Luciferase assays might not reflect on the endogenous events, as the plasmid does not possess the topography the chromatin has. Additionally, since NaBt is a well-known inhibitor of histone deacetylases (HDACi), it has the ability to alter the chromatin topography. Therefore, to determine the endogenous binding of NF- κ B upon NaBt treatment, we performed chromatin immunoprecipitation (ChIP) using antibodies specific to p65 and p50. ChIPs displayed a significant loss of p65 recruitment to the COX-2 promoter in Caco-2 while p50 recruitment did not change (Figure 3.3A). In HT-29, it was p50 recruitment that was significantly increased while p65 recruitment remained unchanged (Figure 3.3B).

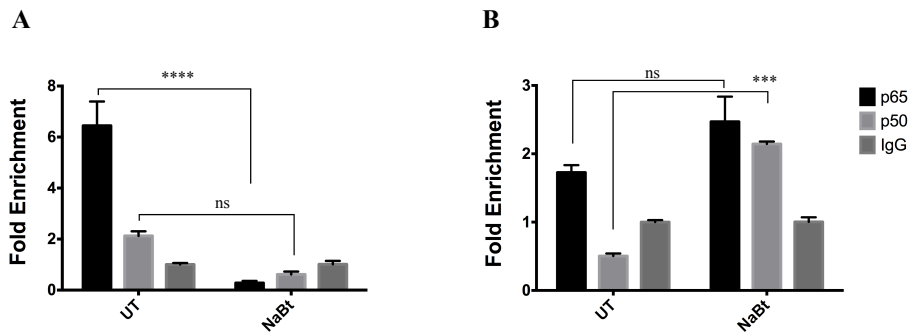


Figure 3.3 ChIP assay using antibodies of p65 and p50, and IgG as negative control in Caco-2 (A) and HT-29 (B). After immunoprecipitating with the indicated antibodies, DNA fragments obtained were used as template in qRT-PCRs for COX-2 promoter region. Data was shown as fold enrichment with respect to IgG.

Since p65 is the subunit possessing the transactivation domain, neither the increase nor the decrease in the COX-2 mRNA and protein levels in Caco-2 or HT-29 cells, respectively, could be attributed to altered NF- κ B transcriptional activity. We also analyzed the activity of AP-1, another important regulator of COX-2 (Kim et al. 2009), via luciferase assay, which did not show a significant difference with treatment (data not shown).

3.3 Post-transcriptional regulation of COX-2 in the presence of NaBt

Since the investigation of the activation of important inflammatory transcription factors NF- κ B and AP-1 did not account for the differential regulation of COX-2 mRNA levels in the two cell lines, we hypothesized that the observed difference was conferred by post-transcriptional regulation.

3.3.1 Alternative polyadenylation of the 3'UTR of COX-2 mRNA

The COX-2 transcript carries two polyadenylation signals on its 3'UTR with regulatory elements in between (Hall-Pogar et al. 2005). The use of the distal polyA signal would result in a longer 3'UTR, with the possibility of greater regulation, while the use of the proximal polyA signal would result in a shorter 3'UTR, which can escape regulation. To determine whether the proximal or the distal polyA signal was used when Caco-2 or HT-29 cells were treated with NaBt, we carried out qRT-PCR amplifications of the longer 3'UTR. The results demonstrated a shift in the preference of distal polyA signal with increasing concentrations of NaBt in Caco-2, indicating the possibility of greater regulation, whereas the polyA signal usage preference did not change significantly in the HT-29 cells (Figure 3.4).

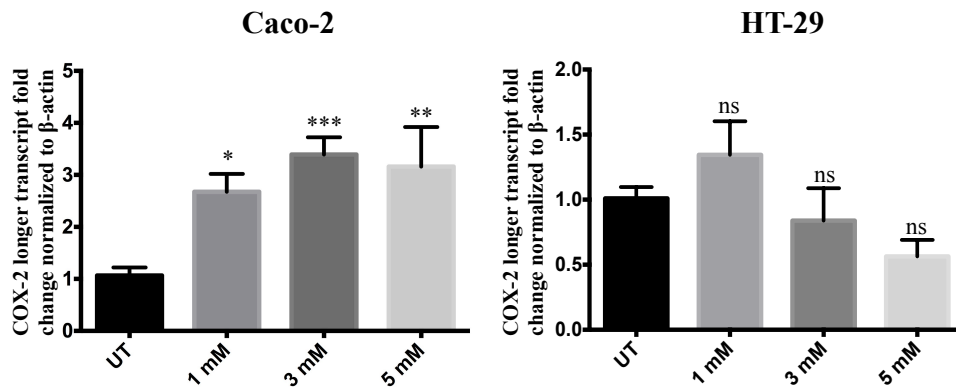


Figure 3.4 qRT-PCR analysis of longer COX-2 transcript using primers against the site between the proximal and distal polyA signals. Significance calculated by comparing to the untreated sample. Data were normalized using β -actin levels.

3.3.2 p38-mediated post-transcriptional regulation of COX-2 mRNA

The differential use of the polyA signal in the 3'UTR of COX-2 in Caco-2 cells indicated that the 3'UTR was indeed regulated in the presence of NaBt. An extensive number of AU-rich elements (AREs, please see section 1.2.4) are located in the 3'UTR of COX-2 mRNA and the initiation of a signaling cascade by the phosphorylation and activation of p38 can induce the mRNA-stabilizing protein HuR (section 1.3.2) while inactivating the destabilizing protein TTP (section 1.3.3). Both HuR and TTP have been shown to bind to the AREs in COX-2 and regulate stability of the mRNA (Young et al. 2009). We therefore investigated the activation of p38 in the two cell lines. In Caco-2 cells, NaBt treatment resulted in an increase of both the Tyr₁₈₂-

phosphorylated and total levels of p38 in the cytoplasm. On the other hand, p38 protein and phosphorylation levels did not vary in HT-29 cells treated with NaBt (Figure 3.5A). To understand whether p38 activation led to changes in the mRNA levels of COX-2, we used SB 202190, a specific inhibitor of p38 activity. After incubation for 30 min, the high mRNA levels of COX-2 due to NaBt treatment in Caco-2 were reduced drastically, whereas a similar difference was not observed in HT-29 cells (Figure 3.5B-C).

To show that the regulation observed was through the 3'UTR of COX-2 mRNA, we transfected Caco-2 and HT-29 cells with a construct of COX-2 3'UTR cloned into psiCheck-2™ dual luciferase vector. Similar to the COX-2 mRNA levels, the normalized *Renilla* luciferase signal from Caco-2 cells increased with NaBt treatment and decreased with SB 202190 treatment. In HT-29 cells, NaBt resulted in a drop in the signal, and SB 202190 treatment did not exhibit a significant effect on the levels (Figure 3.5D-E).

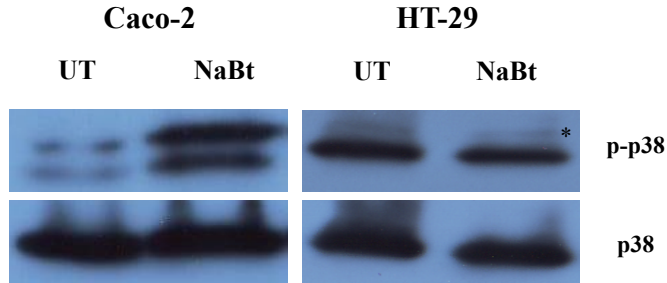
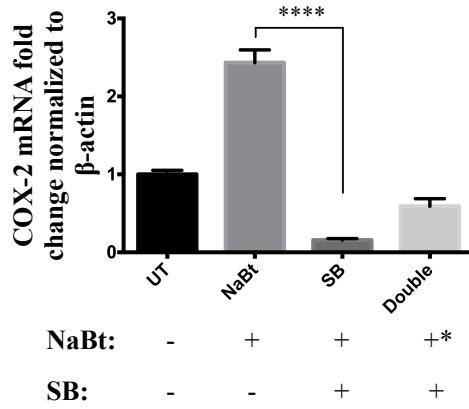
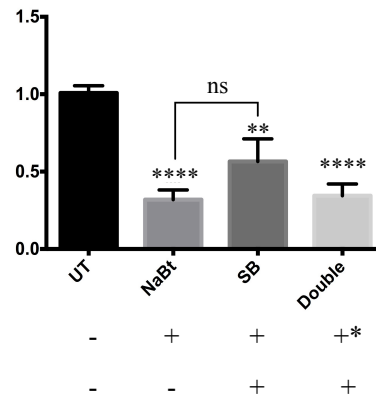
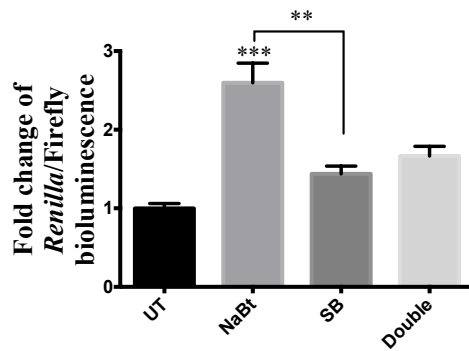
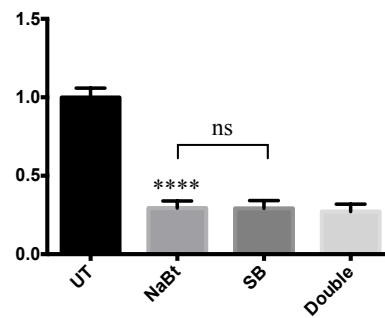
A**B****C****D****E**

Figure 3.5 (A) Phospho-(Tyr₁₈₂) and total p38 levels in cytoplasmic fractions of Caco-2 and HT-29 cell lysates. The upper band in p-p38 (marked with an asterisk) is non-specific. qRT-PCR for COX-2 mRNA in untreated, NaBt-treated, SB 202190-treated (SB) and Double-treated cells of Caco-2 (B) and HT-29 (C). SB and Double samples were pre-treated with NaBt for 48 h. Asterisk indicates that after pre-treatment, the sample was treated with NaBt and SB together. Significance calculated by comparing to the untreated sample. Data were normalized using β -actin. Dual luciferase results using psiCheck-2™ COX-2 3'UTR construct in Caco-2 (D) and HT-29 (E) cells. Data were normalized with respect to bioluminescence of firefly luciferase.

3.4 COX-2 mRNA stability increases upon NaBt treatment

To confirm whether NaBt treatment enhanced mRNA stability differentially in Caco-2 or HT-29 cells, we treated the cells with actinomycin D to inhibit de novo transcription and analyzed COX-2 mRNA levels as a function of time with qRT-PCR and RT-PCR. When Caco-2 cells were treated with NaBt, mRNA stability was observed to be increased relative to the untreated levels (Figure 3.6). This stability was lost when the cells were also treated with SB 202190.

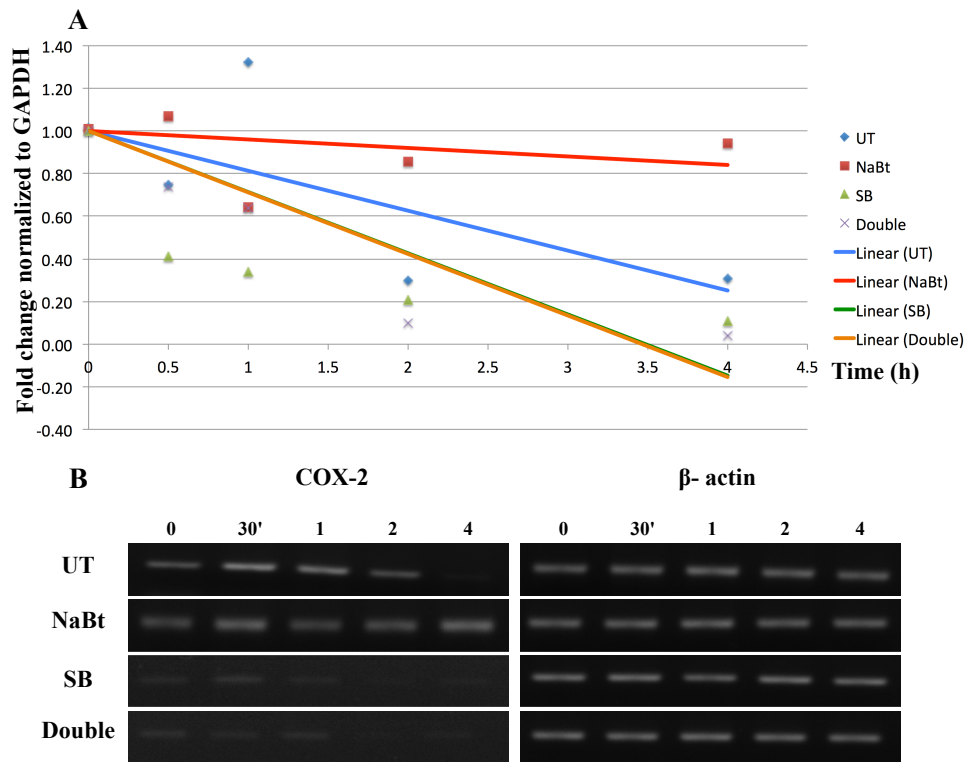


Figure 3.6 Actinomycin D time course of untreated (blue), NaBt-treated (red), SB 202190-treated (green) and Double-treated (orange) Caco-2 cells. After the appropriate treatments, all cells were incubated with actinomycin D (1 μ g/ml) and harvested at the indicated time points. qRT-PCR data (A) were normalized using GAPDH as an internal control. In RT-PCR experiments (B), β -actin was used as loading control.

To determine the stability of COX-2 mRNA in HT-29 cells treated with NaBt, a similar treatment was carried out with actinomycin D. We have observed that, contrary to its effect in Caco-2 cells, NaBt treatment resulted in less stable COX-2 mRNA as compared to the untreated cells (Figure 3.7). Since

SB 202190 treatment showed no change in COX-2 mRNA levels in HT-29 (Figure 3.5C), we did not include it in the HT-29 stability experiments.

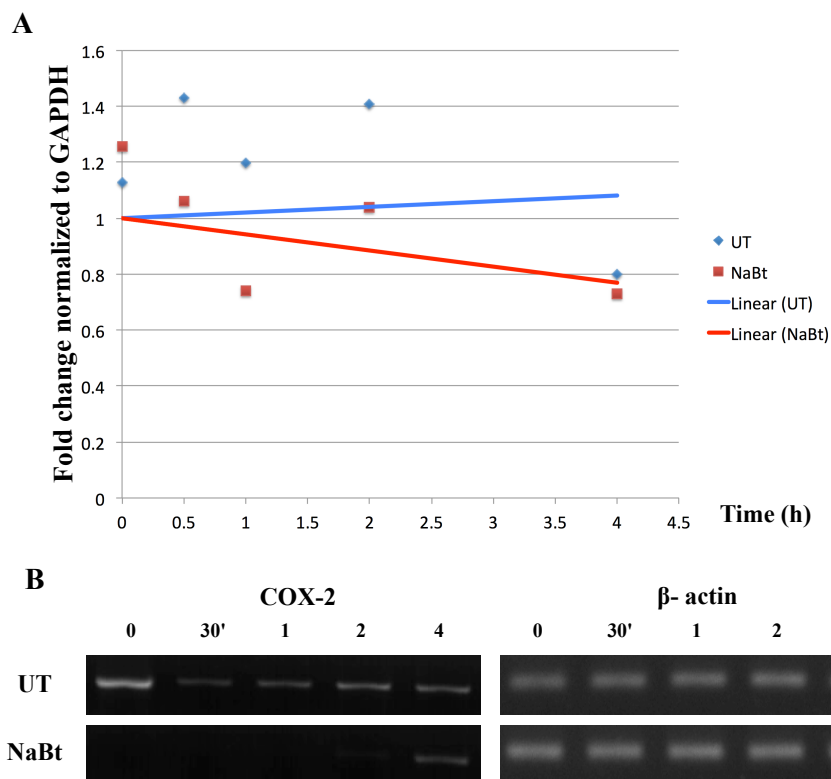


Figure 3.7 Actinomycin D time course of untreated (blue) and NaBt-treated (red) HT-29 cells. After the appropriate treatments, all cells were incubated with actinomycin D (1 μ g/ml) and harvested at the indicated time points. qRT-PCR data (A) were normalized using GAPDH as an internal control. In RT-PCR experiments (B), β -actin was used as loading control.

3.5 HuR and TTP compete for COX-2 mRNA stability in NaBt-treated Caco-2 and HT-29 cells

After the observation that treatment with NaBt not only increased the COX-2 mRNA stability in Caco-2, but also decreased it in HT-29, we wanted to determine the levels of AREBPs HuR and TTP (Figure 3.8). Since HuR is known to be abundant in the nucleus but active in the cytoplasm (Hyeon et al. 2008), we assayed for the HuR levels in the cytoplasmic fraction. We have observed a reduction in the cytoplasmic levels of the HuR protein upon NaBt treatment in both cell lines (Figure 3.8A).

Since the localization of TTP in both the nucleus and cytoplasm have been associated with activation as well as loss of activation depending on the signaling pathways upstream (Brook et al. 2006), we assayed for the total levels of TTP. Unlike HuR, TTP protein levels showed a differential regulation in the two cell lines with a decrease observed in Caco-2 cells with no alteration in HT-29 cells (Figure 3.8B).

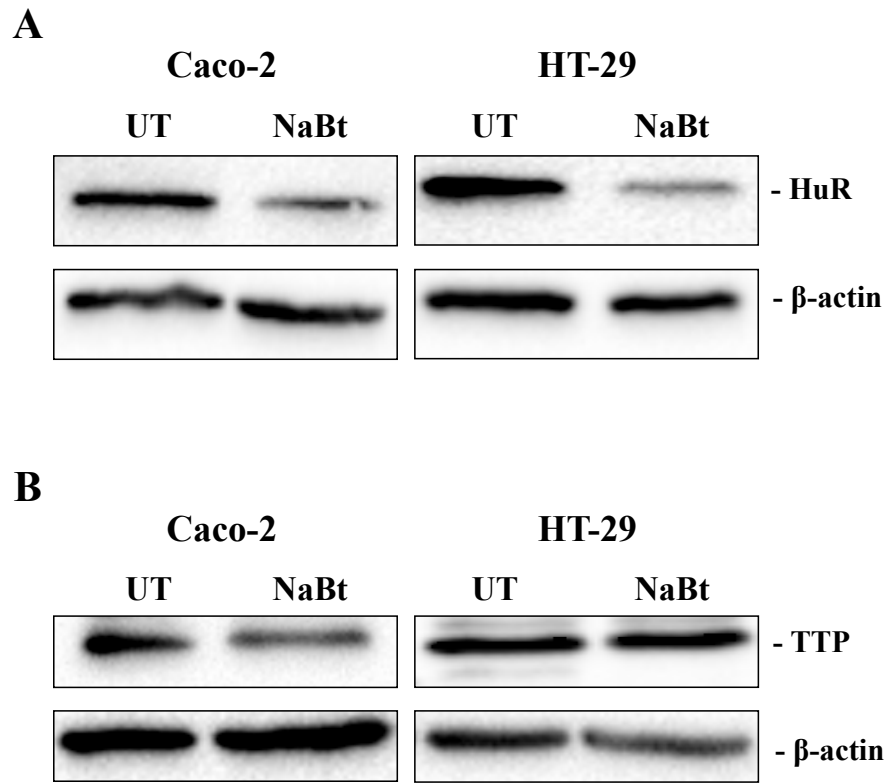


Figure 3.8 HuR levels in the cytoplasmic fraction from untreated or NaBt-treated Caco-2 and HT-29 cells (A). Total TTP levels from untreated or NaBt-treated Caco-2 and HT-29 lysates (B). β -actin was used as protein loading control.

CHAPTER 4

DISCUSSION

In this study, we investigated the effects of the short chain fatty acid NaBt on colon cancer cell lines Caco-2 and HT-29. The concentration of the treatment was selected to be 3 mM, as it is close to the concentration of butyrate in the colon (Wolever et al. 1997). Treatment of Caco-2 cells with 3mM NaBt resulted in increased mRNA and protein expressions of COX-2 (Figure 3.1A-C). On the other hand, HT-29 cells treated with NaBt showed a decrease in COX-2 mRNA and protein levels (Figure 3.1B-C).

NaBt at 3mM has also been used to chemically differentiate colon epithelial cells (Barrasa et al. 2012; Furusawa et al. 2013). Earlier research from our lab has revealed that after 48 h treatment with 3 mM NaBt, HT-29 cells showed an increase in the mRNA levels of differentiation markers such as intestinal alkaline phosphatase (IAP), Hic-5 and Villin (Kucukdemir 2012). Treatment with NaBt also induced colonic differentiation in Caco-2 cells, as identified by the increase in IAP activity (Litvak et al. 1998). Although differentiation was reported to occur in both cell lines (as determined from the increased expression of differentiation markers), however, the differential expression of COX-2 in the two cell lines indicates that the regulation may be independent of differentiation.

Upregulation of COX-2 was observed in cartilage differentiation, however, it is not regarded as a differentiation marker in colon cancer (Ulivi et al. 2008). Interestingly, Ulivi et al. demonstrated that during cartilage differentiation, NF- κ B and p38 pathways were activated, as well. Thus, it can be claimed that treatment with NaBt resulted in activation of a signaling mechanism resembling cartilage differentiation in Caco-2 cells that led to the expression of COX-2, and such a mechanism was not available in the treated HT-29 cells. This study hence affirms that the effect of NaBt, rather than being universal, is exclusive to the cell line or the cell type (Wolter and Stein 2002).

4.1 NaBt and inflammation

It has been a matter of debate whether NaBt induces or reduces inflammation, with the general notion being the inflammatory response was reduced through the inhibition of NF- κ B pathway and the concomitant upregulation of the anti-inflammatory peroxisome proliferator-activated receptor- γ (PPAR γ) (H M Hamer et al. 2008). We investigated the effects of NaBt treatment over NF- κ B, as it is an important regulator of COX-2 expression (will be discussed in the following section). However, since COX-2 is vital in the inflammatory response, regardless of the NF- κ B pathway activity, it is clear that NaBt exhibited differential effects on the expression of inflammatory genes in two colon cancer cell lines. The activity of inflammatory pathways could be reduced, but this might not correlate with the levels of some inflammatory genes downstream, as was the case with COX-2 levels in our study.

4.2 NF- κ B activity in the presence of NaBt

We found by Western blotting that the subcellular localization of the p65 subunit of NF- κ B (with the transactivation domain) showed a difference in the two cell lines where its nuclear presence was induced in Caco-2 cells and slightly reduced in HT-29 cells. The second subunit in the NF- κ B heterodimer, p50, which is known to have inhibitory functions when it translocates to the nucleus as a homodimer (Plaksin, Baeuerle, and Eisenbach 1993), showed a reduction in both cell lines when treated with NaBt (Figure 3.2A).

Nuclear translocation of NF- κ B subunits is usually accompanied by their activity as a transcription factor. When we determined the transcriptional activity of NF- κ B, using a luciferase vector that contains 5 copies of the κ B-binding element, we observed an increase in transcriptional activity in Caco-2 cells and a decrease in HT-29 cells (Figure 3.2B-C). These data corroborated with the Western data described above. However, care must be taken when interpreting data involving expression of luciferase from a plasmid in an experiment where cells are treated with NaBt, an HDAC inhibitor, which can enhance the transcription of genes through the relaxation of the chromatin (Candido, Reeves, and Davie 1978). We therefore carried out chromatin immunoprecipitation using polyclonal antibodies against p65 and p50 to determine the promoter binding of the NF- κ B subunits *in vivo* in the presence or absence of incubation with NaBt. Interestingly, using primers specific for the NF- κ B binding region, we have observed a decrease in the recruitment of p65 and p50 to the promoter of COX-2 in Caco-2 cells (Figure 3.3A). Indeed, qRT-PCRs performed using primers specific to other promoters where NF- κ B is known to bind (i.e. ICAM-1, and VCAM-1) (Xia et al. 2001) showed concomitant results with COX-2 promoter region, indicating lower NF- κ B activity in Caco-2 cells. Therefore, despite the elevated presence of the

subunit p65 in nucleus, the recruitment of NF- κ B to the promoter was reduced in Caco-2 cells, which appears in line with other studies showing a reduction in NF- κ B activity. In HT-29 cells, p65 recruitment was not altered; rather, there seemed to be an increase in the recruitment of p50 subunit (Figure 3.3B), which can be attributed to an inhibition of the transcription of NF- κ B target genes. However, there have been studies showing the p50 homodimers can also induce transcriptional activation, depending on the particular kappa B motifs (Fujita et al. 1992; Cao et al. 2006). Hence, although it was not seen in the context of COX-2 mRNA transcription, whether NF- κ B activity in HT-29 is higher for other inflammatory genes remains to be elucidated.

4.3 Post-transcriptional regulation of COX-2 mRNA

Having observed a dichotomy in the transcriptional regulation of the COX-2 promoter and its mRNA and protein expressions in the NaBt treated cells, we hypothesized that the regulation could be post-transcriptional. The 3'UTR of COX-2 is known to be extensively regulated post-transcriptionally through various mechanisms including microRNAs, alternative polyadenylation, as well as binding of stabilizing or destabilizing proteins to the AU rich elements (Hall-Pogar et al. 2005). We first determined whether the treatment with NaBt resulted in alternative polyadenylation in the COX-2 mRNA.

The 3'UTR of the COX-2 mRNA possesses two polyA signals, which indicate that two COX-2 mRNAs with differing lengths of the polyA tail can be generated. The usage of distal polyA signal would result in a longer 3'UTR, whereas usage of the proximal polyA tail would result in a shorter UTR with potential implications on the extent of regulation through microRNAs or AREBPs (Figure 4.1).

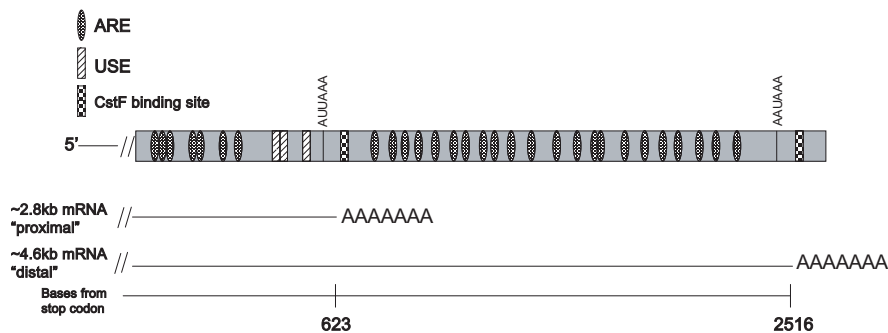


Figure 4.1 The schematic representation of COX-2 3'UTR, with the polyA signals and the AREs shown. The usage of the distal polyA signal generates a transcript that is 1.8 kb longer containing an additional 23 AREs. Adapted from (Hall-Pogar et al. 2005)

We observed that in the presence of NaBt, the distal polyA usage increased in Caco-2 cells, while remaining unchanged in HT-29 cells (Figure 3.4). A longer transcript is usually regarded to be less stable, through post-transcriptional regulation in the higher number of regulatory elements (Sandberg et al. 2008). In the case of NaBt; however, the longer transcript was found to be more stable in Caco-2 cells. A possible explanation would be that the presence of the longer 3'UTR would allow for greater regulation through the availability of more AU-rich elements (Figure 4.1).

4.4 Differential activation of p38 MAPK in the presence of NaBt

The COX-2 transcript, as with the transcripts of other proteins involved in immune functions, is known to be exquisitely regulated through ARE-binding proteins such as HuR and TTP (Young et al. 2009). The activation of these AREBPs is known to be signaled through the p38 MAPK pathway (Fernau et al. 2010). Therefore, we hypothesized that AREBPs were differentially recruited to the 3'UTR of COX-2 mRNA through differential activation of p38. We observed that when the cells were treated with NaBt for 48 h, p38 was activated only in Caco-2 cells, as determined by the phospho-Tyr₁₈₂ levels (Figure 3.5A). Following the NaBt treatment, when the cells were incubated with SB 202190, a specific inhibitor of p38, for 30 min, a strong downregulation of the increased levels of COX-2 mRNA was observed in the Caco-2 cells indicating that the p38 pathway was specifically activated in Caco-2 cells (Figure 3.5B). As expected, a similar treatment of NaBt treated HT-29 cells with SB 202190 did not result in any significant change in COX-2 mRNA indicating that the p38 pathway in this cell line was not stimulated upon NaBt treatment (Figure 3.5C).

SB 202190 binds to the ATP-binding pocket of p38 α/β , thereby inhibiting the kinase activity of the protein, without preventing the phosphorylation of the protein itself (Davies et al. 2000). The inhibitor can bind both the inactive and the active forms of p38. Therefore, the effect of SB 202190 found on Caco-2 cells did not arise from the prevention of p38 phosphorylation. Similarly, the fact that SB 202190 did not change the mRNA levels in HT-29 cells rules out the possibility of a basal activity of p38-driven mRNA stability in HT-29, which would still be affected from SB 202190 treatment.

Considering that p38 activation upon NaBt treatment did not take place in HT-29, it can be postulated that an upstream activator of p38 had a debilitating mutation in this cell line, which prevented the NaBt signal to be

relayed to p38. It would be reasonable to suspect that such a protein must be upstream of both NF- κ B and p38 pathways, as both these pathways were observed to be inactive in HT-29 cells following NaBt treatment. A G-protein from the Rho family, named Rac-1, appears to match the above qualifications, as it can activate both NF- κ B via phosphorylation of I κ B α , as well as p38 through the activation of the MAPK kinase MKK3 (Perona et al. 1997; You et al. 2005; Abcam 2015).

To confirm that the regulation of COX-2 mRNA is via the 3'UTR, we cloned the 3'UTR of COX-2 into psiCheck2 dual luciferase vector, and compared the luciferase signals obtained from untreated, NaBt-treated, SB-treated, and SB+NaBt-treated cells. The effects of treatments on the luciferase signal measured correlated with the COX-2 mRNA levels observed with the respective treatments (Figure 3.5D-E), indicating that 3'UTR of COX-2 was sufficient to confer the observed regulation in the two cell lines. The fact that the fold changes in the luciferase data in Caco-2 and HT-29 cells are quite similar to the fold changes of COX-2 mRNA under the treatments demonstrates that the transcriptional regulation plays little to no role in the NaBt-driven changes in the levels of COX-2 mRNA.

4.5 Acquisition and loss of stability of COX-2 mRNA in Caco-2 and HT-29 cells

To determine whether the differential activation of the p38 pathway in Caco-2 and HT-29 cells had implications on COX-2 mRNA stability in the two cell lines, actinomycin D was used to inhibit de novo transcription, and the COX-2 mRNA levels were examined as a function of time. The most stable pool of COX-2 mRNAs was found when the Caco-2 cells were treated only with NaBt (Figure 3.6). When the cells pre-treated with NaBt were also treated

with SB 202190, the stability of COX-2 mRNA was lower than that of the untreated samples, indicating that there was a degree of basal p38 activity in Caco-2 cells. The COX-2 mRNA stability trendlines for treatment of the cells with SB202190 and for concomitant treatment with SB202190 and NaBt treated cells shown in Figure 3.6 were nearly identical indicating that the drop in stability could not be rescued with the simultaneous treatment with NaBt.

Interestingly, the COX-2 mRNA levels were found to be increased in all the cells treated for 30 min with actinomycin D, regardless of the cell line or the treatment. It is possible to attribute this to the actinomycin D-mediated translocation and activation of HuR (Fan and Steitz 1998; Cell Signaling Technology 2013 ; please see Appendix A). This can be regarded as a failsafe mechanism whereby the stability of the current mRNA pool is increased, which was activated when RNA polymerase II is inhibited by actinomycin D. As will be discussed later, the drop in the cytoplasmic HuR levels in the presence of NaBt is thus compensated for the first 30 min by the effect of actinomycin D, which then interferes with our results. After this initial induction; however, this effect dwindles and the mRNA decay started to become discernible.

Another intriguing, although not unexpected observation from the actinomycin D experiments was that treatment with NaBt resulted in a loss of stabilization of the COX-2 transcripts in HT-29 cells, which could account for the low COX-2 mRNA and protein levels observed when these cells were treated with NaBt. In order to account for this dichotomy in COX-2 stability in Caco-2 and HT-29 cells, we then set out to determine the protein levels of HuR and TTP in the two cell lines. HuR is a protein that is known to stabilize COX-2 mRNA transcripts by binding to ARE rich elements, while TTP is known to enhance the destabilization of COX-2 mRNA through a competition of binding to the same ARE's (Brennan and Steitz 2001). We detected low levels of HuR in the cytoplasm in both of the cell lines, implying the stability of COX-2 mRNA observed in Caco-2 cannot be attributed to HuR alone.

TTP, on the other hand, was found to be downregulated in Caco-2 cells, whereas its level did not change in HT-29. This finding was in line with the mRNA decay experiments: as HT-29 showed a reduction only in the stabilizing AREBP, HuR, the stability of the mRNA was lost when the cells were treated with NaBt. In contrast, in Caco-2 cells, where both the stabilizing and the destabilizing AREBPs, HuR and TTP, were reduced at the same time, the COX-2 mRNA was stabilized. Since TTP dominated HuR in its ability to bind AREs, the overall outcome of the reduction in the levels of both proteins was an increase in the stability of COX-2 mRNA in Caco-2 cells. Consequently, it can be argued that rather than the presence of HuR, it is the absence of TTP that caused the increased stability of COX-2 mRNA in Caco-2 cells; and conversely, it is the absence of HuR that resulted in the loss of stability observed in HT-29 cells.

Another possibility that we have not investigated lies in the origin of TTP. It belongs to TIS11 family of proteins that also includes two other proteins: butyrate response factor-1 and 2 (BRF-1/2), both of which can bind AREs. As their name implies, these zinc-finger proteins were found to respond to NaBt treatment, and can also be regulated by p38 signaling (Sanduja, Blanco, and Dixon 2011). Analogous to TTP, they are almost exclusively nuclear, and upon phosphorylation, translocate to cytoplasm, where they are constrained by 14-3-3 proteins (Stoecklin et al. 2004; Maitra et al. 2008). Thus, the protein levels and the subcellular localization of BRF-1 and BRF-2 might be worth investigating in the Caco-2 and HT-29 cells treated with NaBt.

4.6 p38 activation status as a prognostic marker for treatment with NaBt

The fact that two colon cancer cell lines responded divergently to NaBt in regulating COX-2, a gene that appears to be crucial in the progression of CRC, raises the question of whether it is prudent to use NaBt as an adjuvant for all patients. If our findings coincide with *in vivo* studies, NaBt treatment bears a risk of increasing chronic inflammation in the tumor microenvironment through the upregulation of COX-2, which would exacerbate the disease. Since the observed difference in COX-2 mRNA and protein levels is not related to the HDACi capability of NaBt, the p38 pathway leading to the post-transcriptional regulation of the mRNA is the determining factor in this phenomenon. Although the relevance of the current findings must first be assessed *in vivo*, the Caco-2/HT-29 model of NaBt response may pave the road for a prognostic application where the p38 activation status (or Rac-1, if applicable) of the CRC cells can be investigated from the biopsy samples of a patient, and whether that particular patient must be administered NaBt as therapy could be determined.

CHAPTER 5

CONCLUSION

In this study, the effect of 3 mM NaBt treatment on the regulation of COX-2 in colon cancer cell lines Caco-2 and HT-29 was examined. It was observed that COX-2 mRNA and protein levels showed differential regulation in the two cell lines, with Caco-2 cells exhibiting an induction and HT-29 cells exhibiting a reduction.

At the transcriptional level, the subcellular localization of NF- κ B and its binding to the NF- κ B-response elements through luciferase assays implied the activation of NF- κ B in NaBt-treated cells, however, chromatin immunoprecipitation demonstrated a reduction in the recruitment of p65 and p50 subunits of NF- κ B to the COX-2 promoter. AP-1 was also found to be not related to the observed differences in the mRNA levels.

Ruling out the possibility of the regulation on the transcription level, we hypothesized that the differences observed in COX-2 mRNA levels in the two cell lines could be attributed to post-transcriptional regulation, exerted by the mitogen-activated protein kinase p38. Upon NaBt treatment, the p38 pathway was observed to be activated only in Caco-2 cells; these cells also showed an upregulation of COX-2 mRNA and protein. The enhanced stability of COX-2 mRNA in the presence of NaBt was confirmed with mRNA decay experiments. Additionally, the specificity of 3'UTR-mediated stability was also affirmed.

Based on the protein level differences of the AREBPs HuR and TTP in the two cell lines, a model coherent with our results is proposed, which is as follows:

- Since the levels of HuR, a protein known to stabilize COX-2 mRNA, decreased in the cytoplasm in Caco-2 and HT-29 with NaBt treatment, mRNA stabilization by this AREBP, by itself, is most likely not responsible for the enhanced stabilization of COX-2 mRNA and protein in Caco-2 cells.
- The protein levels of TTP, an AREBP that is known to destabilize the COX-2 mRNA, on the other hand, exhibited a differential regulation in the two cell lines where its protein level was lower in Caco-2 cells, while staying the same in HT-29 cells.
- Taken together, the changes in HuR and TTP levels suggest that, rather than the presence of HuR, the absence of TTP was what caused the stable COX-2 mRNA in Caco-2 cells. Likewise, rather than the elevated presence of TTP, it was the absence of HuR that resulted in the loss of stability observed in HT-29 cells.

Consequently, our data indicate that, aside from the well-known HDACi capacity, NaBt can also regulate the transcriptome through the manipulation of post-transcriptional regulation mechanisms. We hope that the yet unanswered question of why the p38 activation was not detected in HT-29 will, in the future, lead to a prognostic application through which whether a patient should be administered NaBt can be assessed.

CHAPTER 6

FUTURE STUDIES

There are several questions remaining to be answered in this study, which includes, but not limited to:

- Confirmation of whether the stability of COX-2 mRNA is indeed conferred through the absence of TTP. TTP knockdown experiments can be performed to assess whether the COX-2 mRNA levels in Caco-2 cells can be further elevated when the TTP-knockdown cells are treated with NaBt.
- Whether the changes in HuR and TTP protein levels were through the proteasomal degradation. If the ubiquitin-proteasome system is inhibited, it could be interesting to then check the levels of COX-2 mRNA in the presence of NaBt.
- Understanding the functional outcome of the increased COX-2 levels in Caco-2 cells. Pertinent information includes whether it will enhance the cell's survival/proliferation of the cancer cells, as it is usually observed *in vivo*, and thus it is an important question to sought answer for, as this may hold implications regarding NaBt's use as adjuvant.
- Understanding the upstream activator of p38 activity to explain the differential activation of p38 in the two cell lines. This holds

promise in potentially becoming a prognostic marker that would suggest whether a patient will benefit from treatment with NaBt as an adjuvant. If the underlying mechanism of the differential activation is found, this may open a new spectrum of possibilities ranging from the prognostic use to the development of “NaBt-helping” chemicals, which might increase the NaBt response in patients with a low feedback. For this purpose, it might be worth investigating the Rho family protein Rac-1, which is known to be upstream of both NF- κ B and p38 signaling.

REFERENCES

- Abcam. 2015. "Ras Signaling." Accessed January 14.
<http://www.abcam.com/ps/pdf/cancer/ras.pdf>.
- Adcock, I. M., and G. Caramori. 2001. "Cross-Talk between pro-Inflammatory Transcription Factors and Glucocorticoids." *Immunology and Cell Biology* 79: 376–84. doi:10.1046/j.1440-1711.2001.01025.x.
- Aggarwal, Bharat B. 2004. "Nuclear Factor- K B : The Enemy within" 6 (September): 203–8.
- American Cancer Society. 2014. "Colorectal Cancer." Accessed January 12.
<http://www.cancer.org/cancer/colonandrectumcancer/detailedguide/color-ectal-cancer-key-statistics>.
- American Tissue Culture Collection. 2014. "HT-29 ATCC HTB-38 Homo Sapiens Colon Colorectal Adenocarcinoma." Accessed December 17.
http://www.lgcstandards-atcc.org/products/all/HTB-38.aspx?geo_country=tr#generalinformation.
- Badger, A M, J N Bradbeer, B Votta, J C Lee, J L Adams, and D E Griswold. 1996. "Pharmacological Profile of SB 203580, a Selective Inhibitor of Cytokine Suppressive Binding protein/p38 Kinase, in Animal Models of Arthritis, Bone Resorption, Endotoxin Shock and Immune Function." *The Journal of Pharmacology and Experimental Therapeutics* 279: 1453–61.

- Barrasa, Juan I., Angélica Santiago-Gómez, Nieves Olmo, María Antonia Lizarbe, and Javier Turnay. 2012. "Resistance to Butyrate Impairs Bile Acid-Induced Apoptosis in Human Colon Adenocarcinoma Cells via up-Regulation of Bcl-2 and Inactivation of Bax." *Biochimica et Biophysica Acta - Molecular Cell Research* 1823: 2201–9.
doi:10.1016/j.bbamcr.2012.08.008.
- Beelman, C A, and R Parker. 1995. "Degradation of mRNA in Eukaryotes." *Cell* 81: 179–83. doi:10.1016/0092-8674(95)90326-7.
- Bhatt, Dev, and Sankar Ghosh. 2014. "Regulation of the NF-Kappa B Mediated Transcription of Inflammatory Genes." *Frontiers in Immunology*. doi:10.3389/fimmu.2014.00071.
- Brennan, C M, and J A Steitz. 2001. "HuR and mRNA Stability." *Cellular and Molecular Life Sciences : CMLS* 58: 266–77.
doi:10.1007/PL00000854.
- Brook, Matthew, Carmen R Tchen, Tomas Santalucia, Joanne Mcilrath, J Simon C Arthur, Jeremy Saklatvala, and Andrew R Clark. 2006. "Posttranslational Regulation of Tristetraprolin Subcellular Localization and Protein Stability by p38 Mitogen-Activated Protein Kinase and Extracellular Signal-Regulated Kinase Pathways Posttranslational Regulation of Tristetraprolin Subcellular Localizat," Brook, M., Tchen, C. R., Santalucia, T., Mcilrath,. doi:10.1128/MCB.26.6.2408.
- Brosens, L A A, J J Keller, G J A Offerhaus, M Goggins, and F M Giardiello. 2005. "Prevention and Management of Duodenal Polyps in Familial Adenomatous Polyposis." *Gut* 54: 1034–43.
doi:10.1136/gut.2004.053843.
- Bryan, Nicholas, Helen Ahswin, Neil Smart, Yves Bayon, Stephen Wohlert, and John A. Hunt. 2012. "Reactive Oxygen Species (ROS) - A Family of

Fate Deciding Molecules Pivotal in Constructive Inflammation and Wound Healing.” *European Cells and Materials* 24: 249–65.

Buckley, Christopher D, Derek W Gilroy, Charles N Serhan, Brigitta Stockinger, and Paul P Tak. 2013. “The Resolution of Inflammation.” *Nature Reviews. Immunology* 13: 59–66. doi:10.1038/nri3362.

Bultman, SJ. 2014. “Molecular Pathways: Gene–Environment Interactions Regulating Dietary Fiber Induction of Proliferation and Apoptosis via Butyrate for Cancer Prevention.” *Clinical Cancer Research* 20 (4): 799–803. doi:10.1158/1078-0432.CCR-13-2483.

Candido, E P, R Reeves, and J R Davie. 1978. “Sodium Butyrate Inhibits Histone Deacetylation in Cultured Cells.” *Cell* 14: 105–13. doi:10.1016/0092-8674(78)90305-7.

Cao, Shanjin, Xia Zhang, Justin P. Edwards, and David M. Mosser. 2006. “NF-Kappa B1 (p50) Homodimers Differentially Regulate pro- and Anti-Inflammatory Cytokines in Macrophages.” *Journal of Biological Chemistry* 281: 26041–50. doi:10.1074/jbc.M602222200.

Carballo, Ester, Gary S. Gilkeson, and Perry J. Blackshear. 1997. “Bone Marrow Transplantation Reproduces the Tristetraprolin-Deficiency Syndrome in Recombination Activating Gene-2 (-/-) Mice. Evidence That Monocyte/macrophage Progenitors May Be Responsible for TNF?? Overproduction.” *Journal of Clinical Investigation* 100: 986–95. doi:10.1172/JCI119649.

Cebra, John J. 1999. “Influences of Microbiota on Intestinal Immune System Development.” In *American Journal of Clinical Nutrition*. Vol. 69.

- Cell Signaling Technology. 2013. "ELAVL1/HuR (D9W7E) Rabbit mAb Cell Signaling." Accessed January 8.
<http://media.cellsignal.com/pdf/12582.pdf>.
- Chen, Frank, Ann Bin Shyu, and Benjamin L. Shneider. 2011. "Hu Antigen R and Tristetraprolin: Counter-Regulators of Rat Apical Sodium-Dependent Bile Acid Transporter by Way of Effects on Messenger RNA Stability." *Hepatology* 54 (4): 1371–78. doi:10.1002/hep.24496.
- Chen, W, Q Tang, M S Gonzales, and G T Bowden. 2001. "Role of p38 MAP Kinases and ERK in Mediating Ultraviolet-B Induced Cyclooxygenase-2 Gene Expression in Human Keratinocytes." *Oncogene* 20 (29): 3921–26.
- Chrestensen, Carol A., Melanie J. Schroeder, Jeffrey Shabanowitz, Donald F. Hunt, Jared W. Pelo, Mark T. Worthington, and Thomas W. Sturgill. 2004. "MAPKAP Kinase 2 Phosphorylates Tristetraprolin on in Vivo Sites Including Ser178, a Site Required for 14-3-3 Binding." *Journal of Biological Chemistry* 279: 10176–84. doi:10.1074/jbc.M310486200.
- Comes, F, A Matrone, P Lastella, B Nico, F C Susca, R Bagnulo, G Ingravallo, et al. 2007. "A Novel Cell Type-Specific Role of p38alpha in the Control of Autophagy and Cell Death in Colorectal Cancer Cells." *Cell Death and Differentiation* 14: 693–702.
doi:10.1038/sj.cdd.4402076.
- Coussens, Lisa M, and Zena Werb. 2002. "Inflammation and Cancer" 420 (December).
- Cummings, J H. 1981. "Short Chain Fatty Acids in the Human Colon." *Gut* 22: 763–79. doi:10.1136/gut.22.9.763.
- Cummings, J H, E W Pomare, W J Branch, C P Naylor, and G T Macfarlane. 1987. "Short Chain Fatty Acids in Human Large Intestine, Portal,

Hepatic and Venous Blood.” *Gut* 28: 1221–27.

doi:10.1136/gut.28.10.1221.

Davies, S P, H Reddy, M Caivano, and P Cohen. 2000. “Specificity and Mechanism of Action of Some Commonly Used Protein Kinase Inhibitors.” *The Biochemical Journal* 351: 95–105.

doi:10.1517/13543776.11.3.405.

Dean, JLE, Gareth Sully, AR Clark, and Jeremy Saklatvala. 2004. “The Involvement of AU-Rich Element-Binding Proteins in p38 Mitogen-Activated Protein Kinase Pathway-Mediated mRNA Stabilisation.” *Cellular Signalling* 16 (10): 1113–21. doi:10.1016/j.cellsig.2004.04.006.

Dixon, D A, N D Tolley, P H King, L B Nabors, T M McIntyre, G A Zimmerman, and S M Prescott. 2001. “Altered Expression of the mRNA Stability Factor HuR Promotes Cyclooxygenase-2 Expression in Colon Cancer Cells.” *The Journal of Clinical Investigation* 108: 1657–65.

doi:10.1172/JCI12973.

Dixon, Lisa E. Young and Dan A. 2010. “Posttranscriptional Regulation of Cyclooxygenase 2 Expression in Colorectal Cancer.” *Curr Colorectal Cancer Rep* 6: 60–67. doi:10.1007/s11888-010-0044-

3.Posttranscriptional.

Donohoe, Dallas R., Leonard B. Collins, Aminah Wali, Rebecca Bigler, Wei Sun, and Scott J. Bultman. 2012. “The Warburg Effect Dictates the Mechanism of Butyrate-Mediated Histone Acetylation and Cell Proliferation.” *Molecular Cell* 48: 612–26.

doi:10.1016/j.molcel.2012.08.033.

Donohoe, Dallas R., Nikhil Garge, Xinxin Zhang, Wei Sun, Thomas M. O’Connell, Maureen K. Bunger, and Scott J. Bultman. 2011. “The Microbiome and Butyrate Regulate Energy Metabolism and Autophagy

in the Mammalian Colon.” *Cell Metabolism* 13: 517–26.

doi:10.1016/j.cmet.2011.02.018.

DuBois, Raymond N., Michael W. McLane, Kevin Ryder, Lester F. Lau, and Daniel Nathans. 1990. “A Growth Factor-Inducible Nuclear Protein with a Novel Cysteine/histidine Repetitive Sequence.” *Journal of Biological Chemistry* 265: 19185–91.

Eberhart, C E, R J Coffey, A Radhika, F M Giardiello, S Ferrenbach, and R N DuBois. 1994. “Up-Regulation of Cyclooxygenase 2 Gene Expression in Human Colorectal Adenomas and Adenocarcinomas.” *Gastroenterology* 107: 1183–88. doi:S0016508594003033 [pii].

Espel, Enric. 2005. “The Role of the AU-Rich Elements of mRNAs in Controlling Translation.” *Seminars in Cell and Developmental Biology*. doi:10.1016/j.semdb.2004.11.008.

Fan, X C, and J A Steitz. 1998. “HNS, a Nuclear-Cytoplasmic Shuttling Sequence in HuR.” *Proceedings of the National Academy of Sciences of the United States of America* 95: 15293–98. doi:10.1073/pnas.95.26.15293.

Fan, Xinhao Cynthia, and Joan A. Steitz. 1998. “Overexpression of HuR, a Nuclear-Cytoplasmic Shuttling Protein, Increases the in Vivo Stability of ARE-Containing mRNAs.” *EMBO Journal* 17: 3448–60. doi:10.1093/emboj/17.12.3448.

Fernau, Niklas S., Dominik Fugmann, Martin Leyendecker, Kerstin Reimann, Susanne Grether-Beck, Stefanie Galban, Niloofar Ale-Agha, Jean Krutmann, and Lars Oliver Klotz. 2010. “Role of HuR and p38MAPK in Ultraviolet B-Induced Post-Transcriptional Regulation of COX-2 Expression in the Human Keratinocyte Cell Line HaCaT.” *Journal of*

Biological Chemistry 285 (6): 3896–3904.

doi:10.1074/jbc.M109.081430.

Filippova, Natalia, Xiuhua Yang, Peter King, and L. Burt Nabors. 2012. “Phosphoregulation of the RNA-Binding Protein Hu Antigen R (HuR) by Cdk5 Affects Centrosome Function.” *Journal of Biological Chemistry* 287: 32277–87. doi:10.1074/jbc.M112.353912.

Flier, Jeffrey S., Lisa H. Underhill, and Harold F. Dvorak. 1986. “Tumors: Wounds That Do Not Heal.” *New England Journal of Medicine*. doi:10.1056/NEJM198612253152606.

Fodde, R, R Smits, and H Clevers. 2001. “APC, Signal Transduction and Genetic Instability in Colorectal Cancer.” *Nature Reviews. Cancer* 1: 55–67. doi:10.1038/35094067.

Fogh, J, and T Orfeo. 1977. “One Hundred and Twenty-Seven Cultured Human Tumor Cell Lines Producing Tumors in Nude Mice.” *Journal of the National Cancer Institute* 59: 221–26.

Food and Drug Administration. 2015. “List of Bulk Drug Substances That May Be Used in Pharmacy Compounding.” Accessed January 14. <http://www.fda.gov/ohrms/dockets/98fr/cd9817.pdf>.

Fujita, Takashi, Garry P. Nolan, Sankar Ghosh, and David Baltimore. 1992. “Independent Modes of Transcriptional Activation by the p50 and p65 Subunits of NF- κ B.” *Genes and Development* 6: 775–87. doi:10.1101/gad.6.5.775.

Fung, Kim Y C, Leah Cosgrove, Trevor Lockett, Richard Head, and David L Topping. 2012. “A Review of the Potential Mechanisms for the Lowering of Colorectal Oncogenesis by Butyrate.” *The British Journal of Nutrition* 108 (5): 820–31. doi:10.1017/S0007114512001948.

- Furusawa, Yukihiro, Yuuki Obata, Shinji Fukuda, Takaho a Endo, Gaku Nakato, Daisuke Takahashi, Yumiko Nakanishi, et al. 2013. "Commensal Microbe-Derived Butyrate Induces the Differentiation of Colonic Regulatory T Cells." *Nature* 504 (7480). Nature Publishing Group: 446–50. doi:10.1038/nature12721.
- Giovannucci, E., E. B. Rimm, M. J. Stampfer, G. A. Colditz, A. Ascherio, and W. C. Willett. 1994. "Aspirin Use and the Risk for Colorectal Cancer and Adenoma in Male Health Professionals." *Annals of Internal Medicine* 121: 241–46.
- Greenman, Christopher, Philip Stephens, Raffaella Smith, Gillian L Dalgliesh, Christopher Hunter, Graham Bignell, Helen Davies, et al. 2007. "Patterns of Somatic Mutation in Human Cancer Genomes." *Nature* 446: 153–58. doi:10.1038/nature05610.
- Grivennikov, Sergei I, Florian R Greten, and Michael Karin. 2010. "Immunity, Inflammation, and Cancer." *Cell* 140 (6). Elsevier Inc.: 883–99. doi:10.1016/j.cell.2010.01.025.
- Gum, J R, W K Kam, J C Byrd, J W Hicks, M H Sleisenger, and Y S Kim. 1987. "Effects of Sodium Butyrate on Human Colonic Adenocarcinoma Cells. Induction of Placental-like Alkaline Phosphatase." *The Journal of Biological Chemistry* 262: 1092–97.
- Haier, J, M Nasralla, and G L Nicolson. 1999. "Different Adhesion Properties of Highly and Poorly Metastatic HT-29 Colon Carcinoma Cells with Extracellular Matrix Components: Role of Integrin Expression and Cytoskeletal Components." *British Journal of Cancer* 80: 1867–74. doi:10.1038/sj.bjc.6690614.

- Hall-Pogar, Tyra, Haibo Zhang, Bin Tian, and Carol S. Lutz. 2005. "Alternative Polyadenylation of Cyclooxygenase-2." *Nucleic Acids Research* 33 (8): 2565–79. doi:10.1093/nar/gki544.
- Hamer, H M, D Jonkers, K Venema, S Vanhoutvin, F J Troost, and R-J Brummer. 2008. "Review Article: The Role of Butyrate on Colonic Function." *Alimentary Pharmacology & Therapeutics* 27 (2): 104–19. doi:10.1111/j.1365-2036.2007.03562.x.
- Hamer, Henrike M., Daisy M A E Jonkers, Steven A L W Vanhoutvin, Freddy J. Troost, Ger Rijkers, Adriaan de Bruïne, Aalt Bast, Koen Venema, and Robert Jan M Brummer. 2010. "Effect of Butyrate Enemas on Inflammation and Antioxidant Status in the Colonic Mucosa of Patients with Ulcerative Colitis in Remission." *Clinical Nutrition* 29: 738–44. doi:10.1016/j.clnu.2010.04.002.
- Harper, Kelly A, and Alison J Tyson-Capper. 2008. "Complexity of COX-2 Gene Regulation." *Biochemical Society Transactions* 36: 543–45. doi:10.1042/BST0360543.
- Heruth, Daniel P., Gerald W. Zirnstein, John F. Bradley, and Paul G. Rothberg. 1993. "Sodium Butyrate Causes an Increase in the Block to Transcriptional Elongation in the c-Myc Gene in SW837 Rectal Carcinoma Cells." *Journal of Biological Chemistry* 268: 20466–72.
- Hope, Mairi E, Georgina L Hold, Renate Kain, and Emad M El-Omar. 2005. "Sporadic Colorectal Cancer--Role of the Commensal Microbiota." *FEMS Microbiology Letters* 244: 1–7. doi:10.1016/j.femsle.2005.01.029.
- Huang, N, J P Katz, D R Martin, and G D Wu. 1997. "Inhibition of IL-8 Gene Expression in Caco-2 Cells by Compounds Which Induce Histone Hyperacetylation." *Cytokine* 9: 27–36. doi:10.1006/cyto.1996.0132.

- Hyeon, Ho Kim, Kotb Abdelmohsen, Ashish Lal, Rudolf Pullmann, Xiaoling Yang, Stefanie Galban, Subramanya Srikantan, et al. 2008. "Nuclear HuR Accumulation through Phosphorylation by Cdk1." *Genes and Development* 22: 1804–15. doi:10.1101/gad.1645808.
- Karin, Michael, Zheng Gang Liu, and Ebrahim Zandi. 1997. "AP-1 Function and Regulation." *Current Opinion in Cell Biology*. doi:10.1016/S0955-0674(97)80068-3.
- Kiernan, Rosemary, Vanessa Brès, Raymond W M Ng, Marie Pierre Coudart, Selma El Messaoudi, Claude Sardet, Dong Yan Jin, Stephane Emiliani, and Monsef Benkirane. 2003. "Post-Activation Turn-off of NF- κ B-Dependent Transcription Is Regulated by Acetylation of p65." *Journal of Biological Chemistry* 278 (4): 2758–66. doi:10.1074/jbc.M209572200.
- Kim, Su Hyeong, Jung Min Oh, Jae Hong No, Yung Jue Bang, Yong Sung Juhn, and Yong Sang Song. 2009. "Involvement of NF- κ B and AP-1 in COX-2 Upregulation by Human Papillomavirus 16 E5 Oncoprotein." *Carcinogenesis* 30: 753–57. doi:10.1093/carcin/bgp066.
- Kucukdemir, Mumine. 2012. "Investigation of the Effect of Sodium Butyrate-Induced Differentiation on Inflammatory Pathways in Colon Cancer Cells," no. July. Accessed January 19. <http://etd.lib.metu.edu.tr/upload/12614490/index.pdf>.
- Li, Hongwei, Sungmin Park, Britta Kilburn, Mary Anne Jelinek, Agnes Henschen-Edman, Dana W Aswad, Michael R Stallcup, and Ite a Laird-Offringa. 2002. "Lipopolysaccharide-Induced Methylation of HuR, an mRNA-Stabilizing Protein, by CARM1. Coactivator-Associated Arginine Methyltransferase." *The Journal of Biological Chemistry* 277 (47): 44623–30. doi:10.1074/jbc.M206187200.

- Litvak, D. A., B. M. Evers, K. O. Hwang, M. R. Hellmich, T. C. Ko, Jr Townsend C.M., D. W. Mercer, R. A. Hodin, R. G. Postier, and D. I. Soybel. 1998. "Butyrate-Induced Differentiation of Caco-2 Cells Is Associated with Apoptosis and Early Induction of p21(Waf1/Cip1) and p27(Kip1)." *Surgery* 124: 161–70. doi:10.1016/S0039-6060(98)70116-3.
- Liu, Catherine H., Sung H. Chang, Kirsi Narko, Ovidiu C. Trifan, Ming T. Wu, Elizabeth Smith, Christian Haudenschild, Timothy F. Lane, and Timothy Hla. 2001. "Overexpression of Cyclooxygenase-2 Is Sufficient to Induce Tumorigenesis in Transgenic Mice." *Journal of Biological Chemistry* 276: 18563–69. doi:10.1074/jbc.M010787200.
- Lu, Jin-Yu, and Robert J Schneider. 2004. "Tissue Distribution of AU-Rich mRNA-Binding Proteins Involved in Regulation of mRNA Decay." *The Journal of Biological Chemistry* 279: 12974–79. doi:10.1074/jbc.M310433200.
- Maitra, Sushmit, Chu-Fang Chou, Christian A Luber, Kyung-Yeol Lee, Matthias Mann, and Ching-Yi Chen. 2008. "The AU-Rich Element mRNA Decay-Promoting Activity of BRF1 Is Regulated by Mitogen-Activated Protein Kinase-Activated Protein Kinase 2." *RNA (New York, N.Y.)* 14: 950–59. doi:10.1261/rna.983708.
- Malter, J S. 1989. "Identification of an AUUUA-Specific Messenger RNA Binding Protein." *Science* 246: 664–66.
- Mariadason, J M, A Velcich, A J Wilson, L H Augenlicht, and P R Gibson. 2001. "Resistance to Butyrate-Induced Cell Differentiation and Apoptosis during Spontaneous Caco-2 Cell Differentiation." *Gastroenterology* 120: 889–99. doi:10.1053/gast.2001.22472.
- Medzhitov, Ruslan. 2008. "Origin and Physiological Roles of Inflammation." *Nature* 454: 428–35. doi:10.1038/nature07201.

Middleton, Jim, Angela M. Patterson, Lucy Gardner, Caroline Schmutz, and Brian A. Ashton. 2002. "Leukocyte Extravasation: Chemokine Transport and Presentation by the Endothelium." *Blood*. doi:10.1182/blood.V100.12.3853.

Novus Biologicals. 2014. "p38 MAPK Pathway | Novus Biologicals." Accessed December 24. <http://www.novusbio.com/p38mapkpathway.html>.

O'Connell, Ryan M., Dinesh S. Rao, and David Baltimore. 2012. "microRNA Regulation of Inflammatory Responses." *Annual Review of Immunology*. doi:10.1146/annurev-immunol-020711-075013.

Ogawa, Kenji, Feifei Chen, Young-June Kim, and Yan Chen. 2003. "Transcriptional Regulation of Tristetraprolin by Transforming Growth Factor-Beta in Human T Cells." *The Journal of Biological Chemistry* 278: 30373–81. doi:10.1074/jbc.M304856200.

Pahl, H L. 1999. "Activators and Target Genes of Rel/NF-kappaB Transcription Factors." *Oncogene* 18: 6853–66. doi:10.1038/sj.onc.1203239.

Park, Jean Y, Michael H Pillinger, and Steven B Abramson. 2006. "Prostaglandin E2 Synthesis and Secretion: The Role of PGE2 Synthases." *Clinical Immunology (Orlando, Fla.)* 119: 229–40. doi:10.1016/j.clim.2006.01.016.

Paz-priel, Ido, Simone Hounq, Julia Dooher, Alan D Friedman, and Washington Dc. 2013. "Deacetylases from NF- K B p50 Homodimers to Induce NF- K B Target Genes C / EBP α and C / EBP β Oncoproteins Regulate nfkb1 and Displace Histone Deacetylases from NF- B p50 Homodimers to Induce NF- B Target Genes," 4085–94. doi:10.1182/blood-2010-07-294470.

- Peng, Sheila S Y, Chyi Ying A Chen, Nianhua Xu, and Ann Bin Shyu. 1998. "RNA Stabilization by the AU-Rich Element Binding Protein, HuR, an ELAV Protein." *EMBO Journal* 17: 3461–70. doi:10.1093/emboj/17.12.3461.
- Perona, Rosario, Silvia Montaner, Luisa Saniger, Isabel Sánchez-Pérez, Rodrigo Bravo, and Juan Carlos Lacal. 1997. "Activation of the Nuclear Factor- κ B by Rho, CDC42, and Rac-1 Proteins." *Genes and Development* 11: 463–75. doi:10.1101/gad.11.4.463.
- Pfaffl, and Michael W Pfaffl. 2001. "A New Mathematical Model for Relative Quantification in Real-Time RT-PCR." *Nucl. Acids Res.* 29: e45. Accessed January 5. <http://www.pubmedcentral.nih.gov/articlerender.fcgi?artid=55695&tool=pmcentrez&rendertype=abstract>.
- Pinto, Moise, Sylvie Robine-Leon, Marie-Dominique Appay, Michèle Kedinger, Nicole Triadou, Elisabeth Dussaulx, Brigitte Lacroix, et al. 1983. "Enterocyte-like Differentiation and Polarization of the Human Colon Carcinoma Cell Line Caco-2 in Culture." *Biology of the Cell* 47: 323–30.
- Plaksin, D, P A Baeuerle, and L Eisenbach. 1993. "KBF1 (p50 NF-Kappa B Homodimer) Acts as a Repressor of H-2Kb Gene Expression in Metastatic Tumor Cells." *The Journal of Experimental Medicine* 177: 1651–62. doi:10.1084/jem.177.6.1651.
- Ricchi, P, R Zarrilli, A Di Palma, and A M Acquaviva. 2003. "Nonsteroidal Anti-Inflammatory Drugs in Colorectal Cancer: From Prevention to Therapy." *British Journal of Cancer* 88: 803–7. doi:10.1038/sj.bjc.6600829.

- Roelofs, Hennie M J, Rene H M Te Morsche, Bjorn W H van Heumen, Fokko M Nagengast, and Wilbert H M Peters. 2014. "Over-Expression of COX-2 mRNA in Colorectal Cancer." *BMC Gastroenterology* 14 (1): 1. <http://www.biomedcentral.com/1471-230X/14/1>.
- Rouse, John, Philip Cohen, Sylviane Trigon, Michel Morange, Ana Alonso-Llamazares, Daniel Zamanillo, Tim Hunt, and Angel R. Nebreda. 1994. "A Novel Kinase Cascade Triggered by Stress and Heat Shock That Stimulates MAPKAP Kinase-2 and Phosphorylation of the Small Heat Shock Proteins." *Cell* 78: 1027–37. doi:10.1016/0092-8674(94)90277-1.
- Saccani, Simona, Serafino Pantano, and Gioacchino Natoli. 2002. "p38-Dependent Marking of Inflammatory Genes for Increased NF-Kappa B Recruitment." *Nature Immunology* 3: 69–75. doi:10.1038/ni748.
- Sambuy, Y, I De Angelis, G Ranaldi, M L Scarino, A Stammati, and F Zucco. 2005. "The Caco-2 Cell Line as a Model of the Intestinal Barrier : Influence of Cell and Culture-Related Factors on Caco-2 Cell Functional Characteristics." *Cell Biology and Toxicology*, no. 21: 1–26.
- Sandberg, Rickard, J.R. Neilson, Arup Sarma, P.A. Sharp, and C.B. Burge. 2008. "Proliferating Cells Express mRNAs with Shortened 3'untranslated Regions and Fewer microRNA Target Sites." *Science* 320: 1643. doi:10.1126/science.1155390.
- Sanduja, Sandhya, Fernando F. Blanco, and Dan A. Dixon. 2011. "The Roles of TTP and BRF Proteins in Regulated mRNA Decay." *Wiley Interdisciplinary Reviews: RNA*. doi:10.1002/wrna.28.
- Sawaoka, Hitoshi, DA Dixon, JA Oates, and Olivier Boutaud. 2003. "Tristetraprolin Binds to the 3'-Untranslated Region of Cyclooxygenase-2 mRNA a Polyadenylation Variant in a Cancer Cell Line Lacks the

Binding Site.” *Journal of Biological Chemistry* 278 (16): 13928–35.
doi:10.1074/jbc.M300016200.

Scanlan, Pauline D., Fergus Shanahan, Yvonne Clune, John K. Collins, Gerald C. O’Connell, Sullivan, Micheal O’Riordan, Elaine Holmes, Yulan Wang, and Julian R. Marchesi. 2008. “Culture-Independent Analysis of the Gut Microbiota in Colorectal Cancer and Polyposis.” *Environmental Microbiology* 10: 789–98. doi:10.1111/j.1462-2920.2007.01503.x.

Scharek, L, L Hartmann, L Heinevetter, and M Blaut. 2000. “Bifidobacterium Adolescentis Modulates the Specific Immune Response to Another Human Gut Bacterium, Bacteroides Thetaiotaomicron, in Gnotobiotic Rats.” *Immunobiology* 202: 429–41. doi:10.1016/S0171-2985(00)80102-3.

Scott, M L, T Fujita, H C Liou, G P Nolan, and D Baltimore. 1993. “The p65 Subunit of NF-KB Regulates IKB by Two Distinct Mechanisms.” *GENES& DEVELOPMENT*. doi:10.1101/gad.7.7a.1266.

Sears, Cynthia L., and Wendy S. Garrett. 2014. “Microbes, Microbiota, and Colon Cancer.” *Cell Host and Microbe*.
doi:10.1016/j.chom.2014.02.007.

Selleck Chem. 2014. “Sodium-Butyrate-Chemical-Structure.” Accessed December 28. <http://file.selleckchem.com/downloads/struct/Sodium-butyrates-chemical-structure-S1999.gif>.

Sen, R, and D Baltimore. 1986. “Multiple Nuclear Factors Interact with the Immunoglobulin Enhancer Sequences.” *Cell* 46: 705–16.
doi:10.1016/0092-8674(86)90346-6.

- Siegel, Rebecca, Deepa Naishadham, and Ahmedin Jemal. 2012. "Cancer Statistics , 2012." *CA Cancer J Clin* 62: 10–29. doi:10.3322/caac.20138.Available.
- . 2013. "Cancer Statistics, 2013." *CA: A Cancer Journal for Clinicians* 63: 11–30. doi:10.3322/caac.21166.
- Staudt, Louis M. 2010. "Oncogenic Activation of NF-kappaB." *Cold Spring Harbor Perspectives in Biology*. doi:10.1101/cshperspect.a000109.
- Stoecklin, Georg, Tiffany Stubbs, Nancy Kedersha, Stephen Wax, William F C Rigby, T Keith Blackwell, and Paul Anderson. 2004. "MK2-Induced tristetraprolin:14-3-3 Complexes Prevent Stress Granule Association and ARE-mRNA Decay." *The EMBO Journal* 23: 1313–24. doi:10.1038/sj.emboj.7600163.
- Takada, Yasunari, Anjana Bhardwaj, Pravin Potdar, and Bharat B Aggarwal. 2004. "Nonsteroidal Anti-Inflammatory Agents Differ in Their Ability to Suppress NF- J B Activation , Inhibition of Expression of Cyclooxygenase-2 and Cyclin D1 , and Abrogation of Tumor Cell Proliferation," no. April: 9247–58. doi:10.1038/sj.onc.1208169.
- Topping, D L, and P M Clifton. 2001. "Short-Chain Fatty Acids and Human Colonic Function: Roles of Resistant Starch and Nonstarch Polysaccharides." *Physiological Reviews* 81: 1031–64. doi:10.1002/(SICI)1096-8644(199706)103:2<1031::AID-AJPA2>3.0.CO;2-R.
- Traenckner, E Britta-mareen, Heike L Pahl, Thomas Henkel, Kerstin N Schmidt, Sherwin Wilk, and Patrick A Baeuerle. 1995. "Phosphorylation of Human IKB-Ox on Serines 32 and 36 Controls IKB-a Proteolysis and NF-KB Activation in Response to Diverse Stimuli." *EMBO Journal* 14: 2876–83.

- Tsujii, M, and R N DuBois. 1995. "Alterations in Cellular Adhesion and Apoptosis in Epithelial Cells Overexpressing Prostaglandin Endoperoxide Synthase 2." *Cell* 83: 493–501. doi:10.1016/0092-8674(95)90127-2.
- Tsujii, M, S Kawano, and R N DuBois. 1997. "Cyclooxygenase-2 Expression in Human Colon Cancer Cells Increases Metastatic Potential." *Proceedings of the National Academy of Sciences of the United States of America* 94: 3336–40. doi:10.1073/pnas.94.7.3336.
- Ulivi, Valentina, Paolo Giannoni, Chiara Gentili, Ranieri Cancedda, and Fiorella Descalzi. 2008. "p38/NF-kB-Dependent Expression of COX-2 during Differentiation and Inflammatory Response of Chondrocytes." *Journal of Cellular Biochemistry* 104: 1393–1406. doi:10.1002/jcb.21717.
- Vakkila, Jukka, and Michael T Lotze. 2004. "Inflammation and Necrosis Promote Tumour Growth." *Nature Reviews. Immunology* 4: 641–48. doi:10.1038/nri1415.
- Van den Abbeele, Pieter, Clara Belzer, Margot Goossens, Michiel Kleerebezem, Willem M De Vos, Olivier Thas, Rosemarie De Weirdt, Frederiek-Maarten Kerckhof, and Tom Van de Wiele. 2013. "Butyrate-Producing Clostridium Cluster XIVa Species Specifically Colonize Mucins in an in Vitro Gut Model." *The ISME Journal* 7: 949–61. doi:10.1038/ismej.2012.158.
- Van Der Giessen, Kate, Sergio Di-Marco, Eveline Clair, and Imed Eddine Gallouzi. 2003. "RNAi-Mediated HuR Depletion Leads to the Inhibition of Muscle Cell Differentiation." *Journal of Biological Chemistry* 278: 47119–28. doi:10.1074/jbc.M308889200.

- Velázquez, O C, H M Lederer, and J L Rombeau. 1997. "Butyrate and the Colonocyte. Production, Absorption, Metabolism, and Therapeutic Implications." *Advances in Experimental Medicine and Biology* 427: 123–34.
- Waddell, W R, and R W Loughry. 1983. Sulindac for polyposis of the colon., 24 *Journal of surgical oncology* 83–87.
- Wegener, E, and D Krappmann. 2008. "NF-kB Signaling." *Handbook of Experimental Pharmacology*, 237–59. doi:10.1002/wsbm.30.
- Wolever, T. M S, Robert G. Josse, Lawrence A. Leiter, and Jean Louis Chiasson. 1997. "Time of Day and Glucose Tolerance Status Affect Serum Short-Chain Fatty Acid Concentrations in Humans." *Metabolism: Clinical and Experimental* 46: 805–11. doi:10.1016/S0026-0495(97)90127-X.
- Wolter, Freya, and Jürgen Stein. 2002. "Resveratrol Enhances the Differentiation Induced by Butyrate in Caco-2 Colon Cancer Cells." *The Journal of Nutrition* 132: 2082–86.
- Xia, Y F, L P Liu, C P Zhong, and J G Geng. 2001. "NF-kappaB Activation for Constitutive Expression of VCAM-1 and ICAM-1 on B Lymphocytes and Plasma Cells." *Biochemical and Biophysical Research Communications* 289: 851–56. doi:10.1006/bbrc.2001.6067.
- You, Hye Jin, Chang-Hoon Woo, Eun-Young Choi, Sung-Hoon Cho, Yung Joon Yoo, and Jae-Hong Kim. 2005. "Roles of Rac and p38 Kinase in the Activation of Cytosolic Phospholipase A2 in Response to PMA." *The Biochemical Journal* 388: 527–35. doi:10.1042/BJ20041614.
- Young, Lisa E., Sandhya Sanduja, Kristi Bemis-Standoli, Edsel A. Pena, Robert L. Price, and Dan A. Dixon. 2009. "The mRNA Binding Proteins

HuR and Tristetraprolin Regulate Cyclooxygenase 2 Expression During Colon Carcinogenesis.” *Gastroenterology* 136: 1669–79.
doi:10.1053/j.gastro.2009.01.010.

Zarubin, Tyler, and Jiahuai Han. 2005. “Activation and Signaling of the p38 MAP Kinase Pathway.” *Cell Research* 15 (1): 11–18.

Zgouras, Dimitrios, Astrid Wächtershäuser, Daniela Frings, and Jürgen Stein. 2003. “Butyrate Impairs Intestinal Tumor Cell-Induced Angiogenesis by Inhibiting HIF- 1 α Nuclear Translocation.” *Biochemical and Biophysical Research Communications* 300: 832–38. doi:10.1016/S0006-291X(02)02916-9.

Zweibaum, A., M. Pinto, G. Chevalier, E. Dussaulx, N. Triadou, B. Lacroix, K. Haffen, J. L. Brun, and M. Rousset. 1985. “Enterocytic Differentiation of a Subpopulation of the Human Colon Tumor Cell Line HT-29 Selected for Growth in Sugar-Free Medium and Its Inhibition by Glucose.” *Journal of Cellular Physiology* 122: 21–29.
doi:10.1002/jcp.1041220105.

APPENDIX A

CYTOPLASMIC HuR LEVELS UPON ACTINOMYCIN D TREATMENT

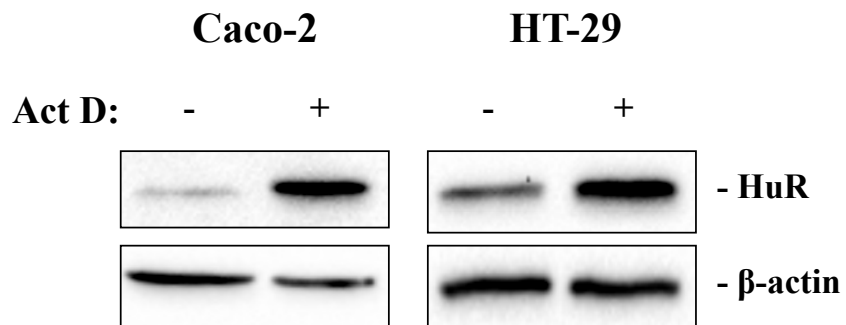
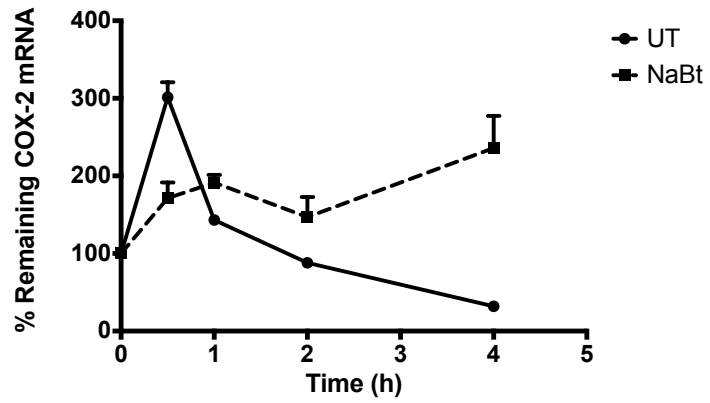


Figure A.1 Cytoplasmic HuR levels in Caco-2 and HT-29 cells treated with 1 $\mu\text{g/ml}$ for 30 min. Note that even though the exposure is quite lower as compared to that in Figure 3.8, actinomycin D-induced levels of cytoplasmic HuR are clearly visible.

Resulting in a massive surge of HuR from nucleus to cytoplasm that was the most prominent in Caco-2 cells, actinomycin D treatment interfered with the mRNA stability results significantly at the first 0.5-1 h.

A



B

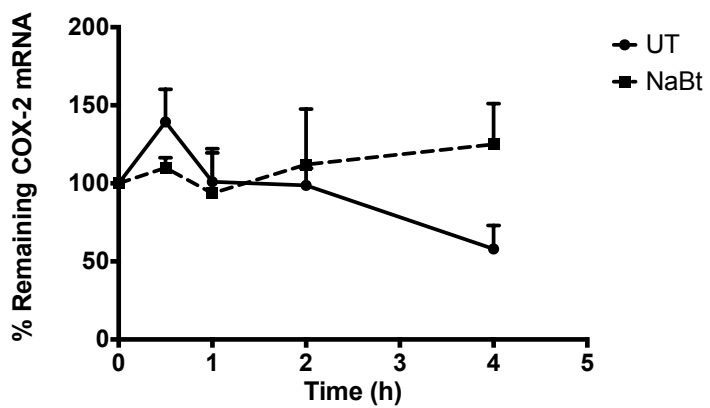


Figure A.2 Results of two representative actinomycin D time course experiments in Caco-2 (A) and HT-29 (B) cells.

The differential increase of COX-2 mRNA levels in the first 30 min in the two cell lines (Figure A.2) also cements our hypothesis of post-transcriptional regulation upon NaBt treatment. As the levels of TTP went down only in Caco-2 cells, the increase of HuR levels mediated by actinomycin D had a much stronger effect on the mRNA levels, as opposed to its effect in HT-29 cells.

APPENDIX B

CLONING OF COX-2 3'UTR TO THE psiCheck2™ VECTOR

The 3'UTR of COX-2 mRNA was cloned amplified from the Mammalian Gene Collection Fully Sequenced Human PTGS2 cDNA (clone ID: 3880850) (Dharmacon) using the below forward and reverse primers:

5'-**GGGCTCGAGAGAACGTTTCGACTGAACT**-3'

5'-**GCGCGCGGCCGCAGAGGAGCTAAATAGCAGTCC**-3'

The introduced NotI and XhoI restriction sites (written bold above) on the fragments and the psiCheck-2 vector were then cut by incubating the following mix at 37°C:

DNA: 15 µl for the amplified fragments; 5 µg for the vector

NotI (Thermo Scientific): 1 µl

XhoI (Thermo Scientific): µl

Buffer O (Thermo Scientific): 2 µl

dH₂O: Up to 20 µl.

The re-ligation of the sticky ends was prevented by dephosphorylation with calf intestinal alkaline phosphatase FastAP (Thermo Scientific) at 37°C as follows:

10X Buffer: 4 µl

CIAP: 1 μ l

DNA: 30 μ l

dH₂O: 5 μ l

PCR purification carried out to remove phosphatase activity. For the ligation reactions, the accurate ng of fragment needed to ligate with 50 ng of vector, the following formula was used:

$$\text{ng insert} = (\text{ng plasmid} * \text{kb insert}) / \text{kb plasmid} * \text{dilution factor}$$

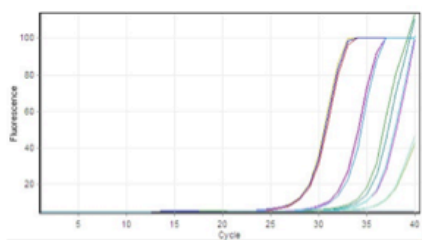
1:3 vector-fragment ratio was adopted in the ligation reactions that was run overnight at 16°C. The reaction was then heat-inactivated at 65°C for 10 min.

For the transformation of XL1-Blue competent cells, 7 μ l of the ligation reaction was added into 100 μ l cell suspension. After 15 min incubation on ice, the cells were heat-shocked at 42°C for 90 sec, and the bacteria were spread on LB (Merck)-Agar (Applichem) plates containing 1X Ampicilin (AppliChem).

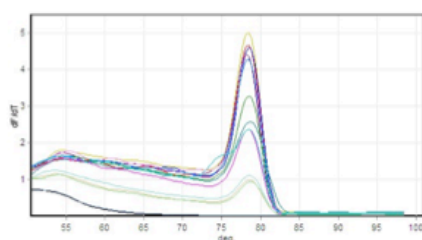
APPENDIX C:

qRT-PCR STANDARD CURVES

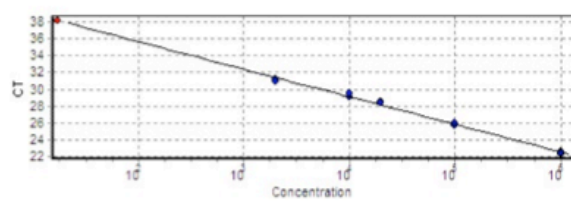
Raw Data For Cycling A.Green



Melt data for Melt A.Green



Standard Curve

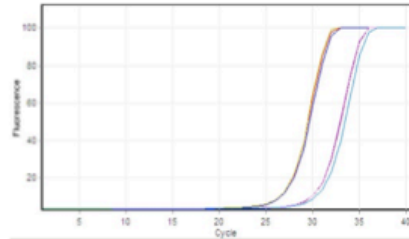


Threshold	0,0384
Left Threshold	1,000
Standard Curve Imported	No
Standard Curve (1)	conc= 10 [^] (-0,307*CT + 12,926)
Standard Curve (2)	CT = -3,260*log(conc) + 42,141
Reaction efficiency (*)	(* = 10 [^] (-1/m) - 1) 1,0264
M	-3,26024
B	42,14109
R Value	0,99575
R ² Value	0,99153
Start normalising from cycle	1
Noise Slope Correction	No
No Template Control Threshold	% 0
Reaction Efficiency Threshold	Disabled
Normalisation Method	Dynamic Tube Normalisation
Digital Filter	Light
Sample Page	Page 1
Imported Analysis Settings	

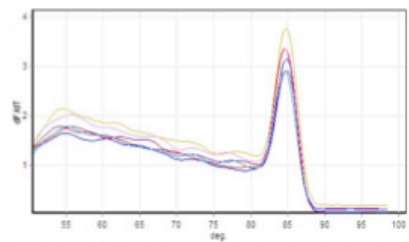
No.	Colour	Name	Type	Ct	Ct Comment	Given Conc (Copies)	Calc Conc (Copies)
1	Red	10-1	Standard	22,55		1.000.000	1.020.229
2	Yellow	10-2	Standard	22,31		1.000.000	1.213.110
3	Blue	10-3	Standard	22,46		1.000.000	1.087.532
4	Purple	100-1	Standard	25,70		100.000	110.112
5	Magenta	100-2	Standard	25,74		100.000	107.551
6	Light Blue	100-3	Standard	25,96		100.000	91.752
7	Dark Green	500-1	Standard	28,56		20.000	14.627
9	Light Green	500-3	Standard	28,41		20.000	16.268
10	Pink	1000-1	Standard	29,55		10.000	7.253
11	Black	1000-2	Standard	29,15		10.000	9.685
12	Cyan	1000-3	Standard	29,46		10.000	7.767
13	Gold	5000-1	Standard	31,02		2.000	2.586
14	Light Green	5000-2	Standard	31,14		2.000	2.368
15	Teal	5000-3	Standard	30,93		2.000	2.753
16	Blue	NTC-1	NTC	38,13			17

Figure C.1 Standard and melt curves used for COX-2 qRT-PCR primers.

Raw Data For Cycling A.Green

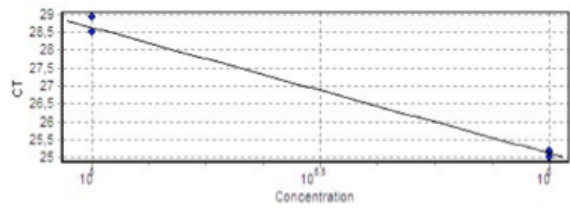


Melt data for Melt A.Green



Threshold	0,3323
Left Threshold	1,000
Standard Curve Imported	No
Standard Curve (1)	conc= 10 ^Y (-0,285*CT + 13,171)
Standard Curve (2)	CT = -3,504*log(conc) + 46,148
Reaction efficiency (*)	(* = 10 ^Y (-1/m) - 1) 0,9293
M	-3,50386
B	46,14837
R Value	0,99617
R^2 Value	0,99235
Start normalising from cycle	1
Noise Slope Correction	No
No Template Control Threshold	% 0
Reaction Efficiency Threshold	Disabled
Normalisation Method	Dynamic Tube Normalisation
Digital Filter	Light
Sample Page	Page 1
Imported Analysis Settings	

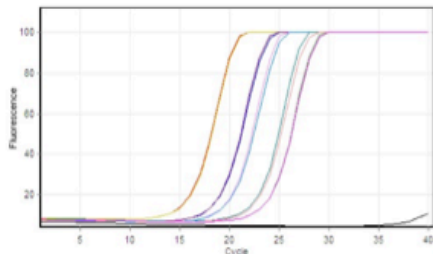
Standard Curve



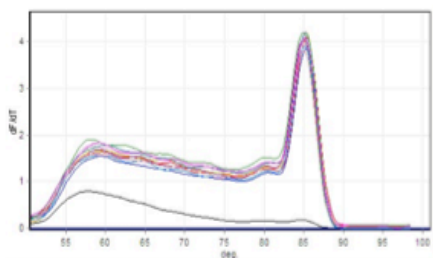
No.	Colour	Name	Type	Ct	Ct Comment	Given Conc (Copies)	Calc Conc (Copies)
1	Red	1:500	Standard	25,02		1000000	1073681,27818643
2	Yellow	1:500	Standard	25,17		1000000	972394,138874988
3	Blue	1:500	Standard	25,19		1000000	957816,440334122
4	Purple	1:5000	Standard	28,48		100000	110096,472911426
5	Pink	1:5000	Standard	28,49		100000	109725,745825562
6	Light Blue	1:5000	Standard	28,92		100000	82778,5953156149

Figure C.2 Standard and melt curves used for β-actin qRT-PCR primers.

Raw Data For Cycling A.Green

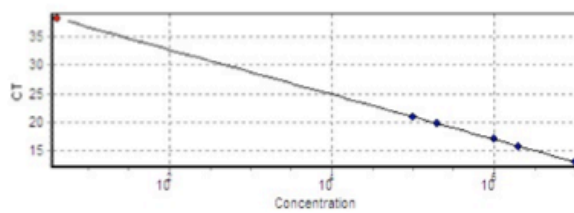


Melt data for Melt A.Green



Threshold	0,1322
Left Threshold	1,000
Standard Curve Imported	No
Standard Curve (1)	conc= 10 [^] (-0,255*CT + 10,342)
Standard Curve (2)	CT = -3,925*log(conc) + 40,588
Reaction efficiency (*)	(* = 10 [^] (-1/m) - 1) 0,79806
M	-3,9246
B	40,58814
R Value	0,99989
R^2 Value	0,99977
Start normalising from cycle	1
Noise Slope Correction	No
No Template Control Threshold	% 0
Reaction Efficiency Threshold	Disabled
Normalisation Method	Dynamic Tube Normalisation
Digital Filter	Light
Sample Page	Page 1
Imported Analysis Settings	

Standard Curve



No.	Colour	Name	Type	Ct	Ct Comment	Given Conc (Copies)	Calc Conc (Copies)
1	Red	10-1	Standard	13,06		10.000.000	10.318.255
2	Yellow	10-2	Standard	13,16		10.000.000	9.751.690
3	Blue	50-1	Standard	15,85		2.000.000	2.014.997
4	Purple	50-2	Standard	15,85		2.000.000	2.010.605
5	Pink	100-1	Standard	17,00		1.000.000	1.024.892
6	Light Blue	100-2	Standard	17,12		1.000.000	952.352
7	Teal	500-1	Standard	19,76		200.000	203.156
8	Light Red	500-2	Standard	19,84		200.000	193.819
9	Light Green	1000-1	Standard	20,95		100.000	101.136
10	Light Purple	1000-2	Standard	20,95		100.000	100.978
11	Black	NC	NTC	38,16			4

Figure C.3 Standard and melt curves used for GAPDH qRT-PCR primers.

APPENDIX D

MINIMUM INFORMATION FOR PUBLICATION OF QUANTITATIVE REAL-TIME PCR EXPERIMENTS GUIDELINES

Table D.1 MIQE guidelines.

ITEM TO CHECK	IMPORTANCE	CHECKLIST
EXPERIMENTAL DESIGN		
Definition of experimental and control groups	E	YES
Number within each group	E	YES
Assay carried out by core lab or investigator's lab?	D	YES
Acknowledgement of authors' contributions	D	NO
NUCLEIC ACID EXTRACTION		
Procedure and/or instrumentation	E	YES
Name of kit and details of any modifications	E	YES
Source of additional reagents used	D	YES
Details of DNase or RNase treatment	E	YES
Contamination assessment (DNA or RNA)	E	NO
Nucleic acid quantification	E	YES
Instrument and method	E	YES
Purity (A260/A280)	D	YES
Yield	D	YES
RNA integrity method/instrument	E	YES
RIN/RQI or Cq of 3' and 5' transcripts	E	NO
Electrophoresis traces	D	N/A
Inhibition testing (Cq dilutions, spike or other)	E	YES
REVERSE TRANSCRIPTION		
Complete reaction conditions	E	YES
Amount of RNA and reaction volume	E	YES
Priming oligonucleotide and concentration	E	YES
Reverse transcriptase and concentration	E	YES
Temperature and time	E	YES
Manufacturer of reagents and catalogue numbers	D	YES
Cqs with and without RT	D	NO
Storage conditions of cDNA	D	YES
qPCR TARGET INFORMATION		
If multiplex, efficiency and LOD of each assay.	E	N/A
Sequence accession number	E	YES
Location of amplicon	D	NO
Amplicon length	E	YES
<i>In silico</i> specificity screen (BLAST, etc)	E	YES
Pseudogenes, retropseudogenes or other homologs?	D	NO
Sequence alignment	D	NO
Secondary structure analysis of amplicon	D	NO
Location of each primer by exon or intron (if applicable)	E	YES
What splice variants are targeted?	E	N/A
qPCR OLIGONUCLEOTIDES		
Primer sequences	E	YES
RTPrimerDB Identification Number	D	N/A
Probe sequences	D	N/A

Table D.1 (continued)

Location and identity of any modifications	E	N/A
Manufacturer of oligonucleotides	D	YES
Purification method	D	NO
qPCR PROTOCOL		
Complete reaction conditions	E	YES
Reaction volume and amount of cDNA/DNA	E	YES
Primer, (probe), Mg ⁺⁺ and dNTP concentrations	E	YES
Polymerase identity and concentration	E	YES
Buffer/kit identity and manufacturer	E	YES
Exact chemical constitution of the buffer	D	N/A
Additives (SYBR Green I, DMSO, etc.)	E	YES
Manufacturer of plates/tubes and catalog number	D	YES
Complete thermocycling parameters	E	YES
Reaction setup (manual/robotic)	D	NO
Manufacturer of qPCR instrument	E	YES
qPCR VALIDATION		
Evidence of optimization (from gradients)	D	YES
Specificity (gel, sequence, melt, or digest)	E	YES
For SYBR Green I, C _q of the NTC	E	YES
Standard curves with slope and y-intercept	E	YES
PCR efficiency calculated from slope	E	YES
Confidence interval for PCR efficiency or standard error	D	N/A
r ² of standard curve	E	YES
Linear dynamic range	E	YES
C _q variation at lower limit	E	YES
Confidence intervals throughout range	D	N/A
Evidence for limit of detection	E	YES
If multiplex, efficiency and LOD of each assay.	E	N/A
DATA ANALYSIS		
qPCR analysis program (source, version)	E	YES
C _q method determination	E	YES
Outlier identification and disposition	E	N/A
Results of NTCs	E	YES
Justification of number and choice of reference genes	E	YES
Description of normalization method	E	YES
Number and concordance of biological replicates	D	YES
Number and stage (RT or qPCR) of technical replicates	E	YES
Repeatability (intra-assay variation)	E	YES
Reproducibility (inter-assay variation, %CV)	D	NO
Power analysis	D	NO
Statistical methods for result significance	E	YES
Software (source, version)	E	YES
C _q or raw data submission using RDML	D	N/A

E: Essential information, D: Desirable information, N/A: Not applicable

APPENDIX E

CONTENTS OF BUFFERS USED FOR WESTERN BLOT EXPERIMENTS

6X Sample Loading Buffer

12% SDS, 30% β -mercaptoethanol, 30% glycerol, 0.012% Bromophenol Blue, 0.375 M Tris-HCl pH 6.8

PBS-T

8 g NaCl, 0.27 g KH_2PO_4 , 3.58 g $\text{Na}_2\text{HPO}_4 \cdot 12\text{H}_2\text{O}$; pH adjusted to 7.4, autoclaved, and 0.1% Tween-20 added before use.

TBS-T

50 mM Tris-HCl pH 7.4, 150 mM NaCl; autoclaved, and 0.1% Tween-20 added before use.

10X Blotting Buffer

30.3 g Trizma Base (0.25 M), 144 g glycine (1.92 M); pH adjusted to 8.3 in 1 L dH_2O .

Transfer Buffer (2 L)

400 ml methanol, 200 ml 10X Blotting Buffer, 1400 ml water

SDS-PAGE Buffer

25 mM Tris, 190 mM glycine, 0.1% SDS

12% Separating Gel Mix

4.3 ml dH₂O, 3.8 ml 10% SDS+1.5 M Tris-HCl pH 8.8, 6.7 ml of acrylamide+bisacrylamide (30%), 150 µl APS, 20 µl TEMED.

4% Stacking Gel Mix

4.7 ml dH₂O, 2 ml 10% SDS+1.5 M Tris-HCl pH 6.8, 1.2 ml of acrylamide+bisacrylamide (30%), 50 µl APS, 10 µl TEMED.

Mild Stripping Buffer

15 g glycine, 1 g SDS, 10 ml Tween-20; pH adjusted to 2.2 in 1 L dH₂O.

Harsh Stripping Buffer

100 mM β-mercaptoethanol, 2% SDS, 62.5 mM Tris-HCl pH 6.8

APPENDIX F

MAPS OF VECTORS USED IN THIS STUDY

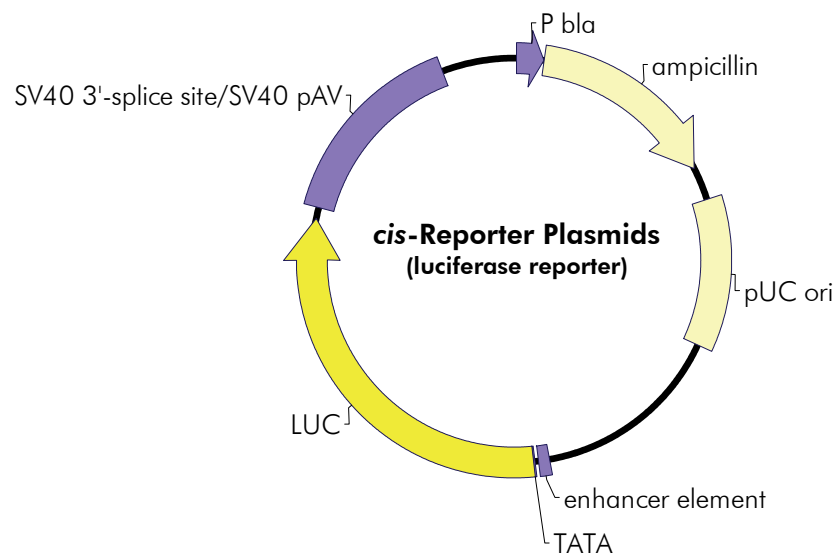


Figure F.1 The base map for PathDetect *cis*-Reporter plasmids (Agilent Technologies). The NF- κ B PathDetect plasmid used in this study possesses five tandem repeats of the NF- κ B response element (TGGGGACCTTTCCGC).

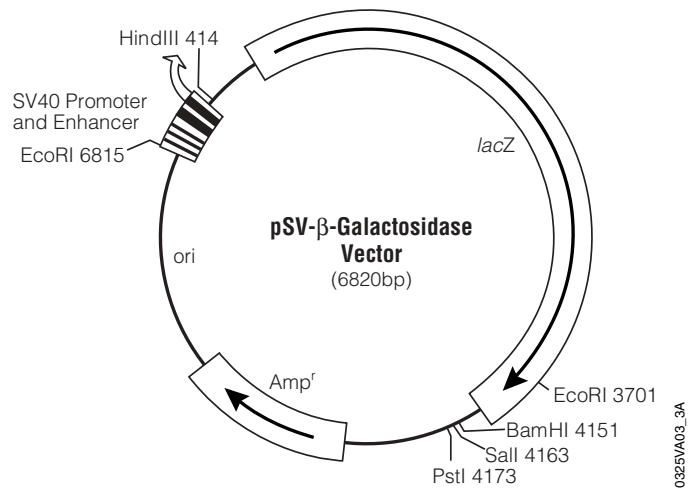


Figure F.2 pSV-β-Galactosidase (Promega).

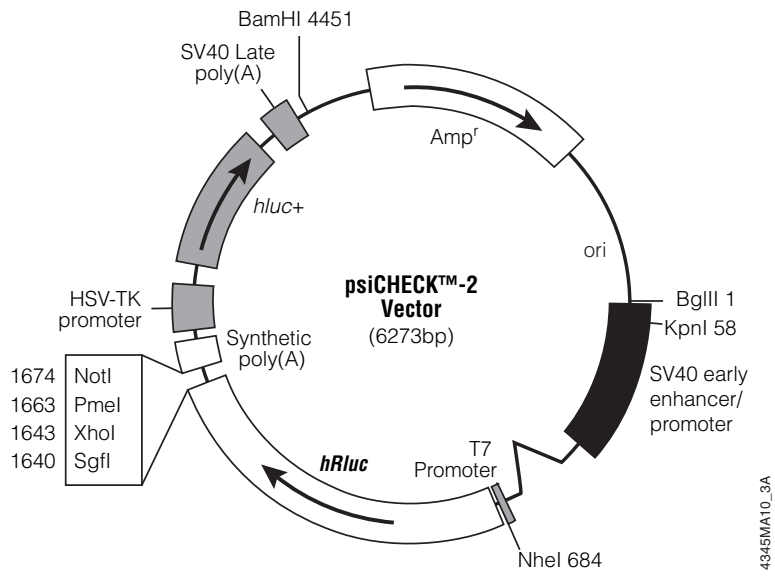


Figure F.3 psiCHECK™-2 (Promega).